U.S. DEPARTMENT OF COMMERCE
National Technical Information Service

PB-280 199

Burner Design Criteria for NOx Control from Low-BTU Gas Combustion: Volume II. Elevated Fuel Temperature

Institute of Gas Technology, Chicago, Ill

Prepared for

Industrial Environmental Research Lab, Research Triangle Park, N C

Dec 77

PB 280 199

EPA U.S. Environmental Protection Agency
Office of Research and Development

Industrial Environmental Research
Laboratory
Research Triangle Park, North Carolina 27711

EPA-600/7-77-094b
December 1977

BURNER DESIGN CRITERIA FOR NO_x CONTROL FROM LOW-BTU GAS COMBUSTION: VOLUME II. ELEVATED FUEL TEMPERATURE

Interagency
Energy-Environment
Research and Development
Program Report

REPRODUCED BY
NATIONAL TECHNICAL
INFORMATION SERVICE
U.S. DEPARTMENT OF COMMERCE
SPRINGFIELD, VA. 22161

RESEARCH REPORTING SERIES

Research reports of the Office of Research and Development, U.S. Environmental Protection Agency, have been grouped into nine series. These nine broad categories were established to facilitate further development and application of environmental technology. Elimination of traditional grouping was consciously planned to foster technology transfer and a maximum interface in related fields. The nine series are:

1. Environmental Health Effects Research
2. Environmental Protection Technology
3. Ecological Research
4. Environmental Monitoring
5. Socioeconomic Environmental Studies
6. Scientific and Technical Assessment Reports (STAR)
7. Interagency Energy-Environment Research and Development
8. "Special" Reports
9. Miscellaneous Reports

This report has been assigned to the INTERAGENCY ENERGY-ENVIRONMENT RESEARCH AND DEVELOPMENT series. Reports in this series result from the effort funded under the 17-agency Federal Energy/Environment Research and Development Program. These studies relate to EPA's mission to protect the public health and welfare from adverse effects of pollutants associated with energy systems. The goal of the Program is to assure the rapid development of domestic energy supplies in an environmentally-compatible manner by providing the necessary environmental data and control technology. Investigations include analyses of the transport of energy-related pollutants and their health and ecological effects; assessments of, and development of, control technologies for energy systems; and integrated assessments of a wide range of energy-related environmental issues.

REVIEW NOTICE

This report has been reviewed by the participating Federal Agencies, and approved for publication. Approval does not signify that the contents necessarily reflect the views and policies of the Government, nor does mention of trade names or commercial products constitute endorsement or recommendation for use.

This document is available to the public through the National Technical Information Service, Springfield, Virginia 22161.

TECHNICAL REPORT DATA
(Please read Instructions on the reverse before completing)

1. REPORT NO.	2.	3. RECIPIENT'S ACCESSION NO.
EPA-600/7-77-094b		PB280199

4. TITLE AND SUBTITLE	5. REPORT DATE
Burner Design Criteria for NOx Control from Low-Btu Gas Combustion; Volume II. Elevated Fuel Temperature	December 1977
	6. PERFORMING ORGANIZATION CODE
7. AUTHOR(S)	8. PERFORMING ORGANIZATION REPORT NO.
Donald R. Shoffstall and Richard T. Waibel	
9. PERFORMING ORGANIZATION NAME AND ADDRESS	10. PROGRAM ELEMENT NO.
Applied Combustion Research Institute of Gas Technology IIT Center, 3424 South State Street Chicago, Illinois 60616	EHE624a
	11. CONTRACT/GRANT NO.
	68-02-1360
12. SPONSORING AGENCY NAME AND ADDRESS	13. TYPE OF REPORT AND PERIOD COVERED
EPA, Office of Research and Development Industrial Environmental Research Laboratory Research Triangle Park, NC 27711	Final; 10/76-10/77
	14. SPONSORING AGENCY CODE
	EPA/600/13

15. SUPPLEMENTARY NOTES IERL-RTP project officer is David G. Lachapelle, Mail Drop 65, 919/514-2236.

16. ABSTRACT **The report gives results** of a program to provide quantitative data on combustion emissions from high-temperature low-Btu gas. It complements a recently completed EPA project that evaluated emissions resulting from the burning of ambient-temperature low-Btu gas. The experimental results were gathered from a pilot-scale furnace fired with a movable-vane boiler burner at a heat input of 0.66 MW (2.25 million Btu/hr). The gases tested in this program--Winkler oxygen, Koppers-Totzek oxygen, and Wellman-Galusha air--ranged from 5.8 MJ/cu m (156 Btu/cu ft) to 9.9 MJ/cu m (266 Btu/cu ft). Measurements were made of NO emissions, temperatures within the flame, and flame emissivity. A mathematical model was used to predict the efficiencies of the furnace with the various fuels; the model agreed well with the experimental measurements. The NO emissions of the gases tested were ordered by the adiabatic flame temperature.

17. KEY WORDS AND DOCUMENT ANALYSIS

a. DESCRIPTORS		b. IDENTIFIERS/OPEN ENDED TERMS	c. COSATI Field/Group	
Air Pollution	Design	Air Pollution Control	13B	
Nitrogen Oxides	High-temperature Tests	Stationary Sources	07B	
Manufactured Gas		Low-Btu Gases	21D	14B
Natural Gas	Flames			
Combustion Control	Emissivity		21B	
Burners			13A	

18. DISTRIBUTION STATEMENT	19. SECURITY CLASS (This Report)	21. NO. OF PAGES
Unlimited	Unclassified	87
	20. SECURITY CLASS (This page)	22. PRICE
	Unclassified	PC A05/MF A01

EPA Form 2220-1 (9-73)

EPA-600-7-77-094b
December 1977

BURNER DESIGN CRITERIA FOR NO_x CONTROL FROM LOW-BTU GAS COMBUSTION: VOLUME II. ELEVATED FUEL TEMPERATURE

by

Donald R. Shoffstall and Richard T. Waibel

Applied Combustion Research
Institute of Gas Technology
IIT Center, 3424 South State Street
Chicago, Illinois 60616

Contract No. 68-02-1360
Program Element No. EHE624a

EPA Project Officer: David G. Lachapelle

Industrial Environmental Research Laboratory
Office of Energy, Minerals and Industry
Research Triangle Park, N.C. 27711

Prepared for

U.S. ENVIRONMENTAL PROTECTION AGENCY
Office of Research and Development
Washington, D.C. 20460

ABSTRACT

This program was initiated to provide quantitative data on combustion emissions from "high-temperature," low-Btu gas. It was intended to complement a recently completed EPA project that evaluated emissions resulting from the burning of "ambient-temperature," low-Btu gas. All the experimental results were gathered from a pilot-scale furnace fired with a moveable vane boiler burner at a heat input of 0.66 MW (2,250,000 Btu/hr). The gases tested in this program, Winkler oxygen (WO), Koppers-Totzek oxygen (KTO),and Wellman-Galusha air (WGA), ranged from 5.8 MJ/m^3 (156 Btu/ft^3) to 9.9 MJ/m^3 (266 Btu/ft^3). Measurements were made of NO emissions, temperatures within the flame, and flame emissivity. A mathematical model was used to predict the efficiencies of the furnace with the various fuels and the model agreed well with the experimental measurements. The NO emissions of the gases tested were ordered by the adiabatic flame temperature.

TABLE OF CONTENTS

	Page
INTRODUCTION	1
SUMMARY	4
DESCRIPTION OF TEST FACILITY	5
Gas Generating System	5
Pilot-Scale Furnace	8
Analytical Test Equipment	15
NO and NO_2 Instrumentation	17
CO, CH_4, and CO_2 Measurements	18
Oxygen Measurements	18
Chromatographic Measurements	18
EXPERIMENTAL PLAN	24
NO Emission Levels	26
Temperature Profiles	41
Flame Emissivity Determination	42
DATA CORRELATION	59
NO Emissions	59
Furnace Performance	59
Mathematical Model of Furnace Performance	66
In-the-Flame Analysis	73
CONVERSION TABLE	76

FIGURES

No.		Page
1	Schematic Diagram of IGT Gas-Generating System	6
2	Gas-Generating System	7
3	Rectangular Test Furnace	9
4	Removable Sidewall Furnace Panels for Interior Flame Probing	10
5	Overall System Schematic Diagram of Rectangular Test Furnace	11
6	Radiant Tube Preheater for Main Furnace Combustion Air	13
7	Flue-Gas Cooler	14
8	Control Room Facility and Analytical Instrumentation	16
9	Gas-Sampling Probe Head for Nonparticulate Flue Gases	20
10	Modified IFRF Temperature Probe	21
11	General Probe Holder	22
12	Pyroelectric Radiometer (Used for Emissivity Measurement)	23
13	Diagram of Movable-Vane Boiler Burner	25
14	Method of Measuring Movable-Vane Angle for Boiler Burner	25
15	NO Emissions Versus Fuel Gas Preheat With Winkler Oxygen Gas	27
16	NO Emissions Versus Secondary Air Preheat With Winkler Oxygen Gas	28
17	NO Emissions Versus Secondary Air Preheat With Natural Gas	29
18	NO Emissions Versus FGR for "Ambient" Winkler Oxygen Fuel	31

FIGURES, Cont.

No.		Page
19	NO Emissions Versus FGR for Winkler Oxygen Preheated to 800°F	32
20	NO Emissions Versus Fuel Gas Preheat With Koppers-Totzek Oxygen Gas	33
21	NO Emissions Versus Secondary Air Preheat With Koppers-Totzek Oxygen Gas	34
22	NO Emissions Versus FGR for "Ambient" Koppers-Totzek Oxygen Fuel	36
23	NO Emissions Versus FGR for Koppers-Totzek Oxygen Fuel Preheated to 800°F	37
24	NO Emissions Versus Fuel Gas Preheat With Wellman-Galusha Air Gas	38
25	NO Emissions Versus Secondary Air Preheat With Wellman-Galusha Air Gas	39
26	Arrhenius Plot of ln [NO] Versus Reciprocal of the Adiabatic Flame Temperature	40
27	Average Gas Temperature Profile for Natural Gas With a 45-Degree Vane Rotation	43
28	Average Gas Temperature Profile for "Ambient" Koppers-Totzek Oxygen Gas With a 45-Degree Vane Rotation	44
29	Average Gas Temperature Profile for Preheated Koppers-Totzek Oxygen Gas With a 45-Degree Vane Rotation	45
30	Average Gas Temperature Profile for Preheated Koppers-Totzek Oxygen Gas With 15% FGR With a 45-Degree Vane Rotation	46
31	Refractory Emissivity Versus Refractory Temperature	49
32	Gas Emissivity Versus Axial Position for Natural Gas	51
33	Gas Emissivity for "Ambient" Koppers-Totzek Oxygen Gas	52

FIGURES, Cont.

No.		Page
34	Gas Emissivity Versus Axial Position for Preheated Koppers-Totzek Oxgyen Gas	53
35	Gas Emissivity Versus Axial Position for Preheated Koppers-Totzek Oxygen Gas With 15% FGR	54
36	Flame Flow Pattern Tested	56
37	NO Emissions Versus Firing Density for the Pilot-Scale Furnace	60
38	Comparison of IGT Experimental and B&W Calculated Furnace Efficiencies	69
39	Comparison of Experimental and Well Stirred Speckled-Wall Model Calculated Furnace Efficiencies	71
40	Variation of Well Stirred Approximation with Adiabatic Radiance	72
41	Comparison of Experimental and Non-Well Stirred Speckled-Wall Model Calculated Furnace Efficiencies	74

TABLES

No.		Page
1	Synopsis of Furnace Operating Conditions and Test Results for a 45-Degree Vane Angle	2
2	Species Concentrations, Adiabatic Flame Temperatures, and Gross Heating Value (Wet) for Medium- and Low-Btu Gases	3
3	Preheater Tube Lengths Versus Preheat Temperature for Gases Tested	8
4	Calculated and Measured Emissivities	58
5	Projected NO Emission Levels for a Utility Boiler	61
6	Pilot-Scale Furnace Efficiencies for Preheated Fuel Gases	62
7	B&W Calculated Boiler Efficiencies Using IGT Data	63
8	Calculated and Measured Radiant Section Exit Gas Temperature and Emissivities	65
9	Comparison of Measured and Calculated Furnace Efficiencies	75
10	Comparison of Calculated Emissivities	75

INTRODUCTION

The objective of this work was to provide and evaluate quantitative data on the environmental quality of effluent combustion products when retrofitting a utility boiler burner with "high-temperature," low-Btu gas. This program was intended to compliment a recently completed EPA project, which evaluated the emissions resulting from burning "ambient temperature," low-Btu gases.

Work is currently being done by government and industry to develop high-temperature, post gasification sulfur cleanup systems. This is an attractive development because it enables utilization of the product gas's sensible heat. It is not obvious what effect these high temperature gases will have on NO emissions, since the higher fuel temperature which results from using a high-temperature, sulfur-removal system does not necessarily result in a higher adiabatic flame temperature, due to the increased water vapor content of the gas. The steam produced during gasification is not removed by cooling as with conventional cleanup systems.

To ensure the immediate relevance of the program's results, only gas compositions from commercially available coal conversion processes (Lurgi, Koppers-Totzek, Winkler, and Wellman-Galusha) were considered. The fuel gases were selected for testing based on the results of emission trials with ambient temperature fuel gas. A summary of these test results is presented in Table 1. The gases selected for "high-temperature" testing were Winkler oxygen (WO), Koppers-Totzek oxygen (KTO), and Wellman-Galusha air (WGA). Koppers-Totzek oxygen and Winkler oxygen gases had emissions equivalent to or greater than those from natural gas combustion. Wellman-Galusha air gas had the highest level of NO emissions of the air gases tested. Table 2 presents species concentrations for "high-temperature" and "ambient-temperature," low-Btu gases. Emission trials were conducted with these fuel gases preheated to 400°, 800°, and 1200°F. These fuel gases were tested to evaluate changes in the level of NO emissions, temperatures within the flame, flame emissivities, and furnace efficiencies when substituted for natural gas on a utility boiler. The actual testing was done on a pilot-scale test furnace modeled to simulate the radiant (furnace) section of a boiler.

Table 1. SYNOPSIS OF FURNACE OPERATING CONDITIONS AND TEST RESULTS FOR A 45-DEGREE VANE ANGLE (Part 1)

Fuel	Gross heating value, Btu/SCF	Adiabatic flame temp, °F	H_2/CO ratio	Fuel input vel, ft/s	Combustion air inlet vel, ft/s
Natural gas	1035.0	3337	--	100.6	53.3
Lurgi oxygen	285.4	3164	2.2	100.0	51.2
Winkler oxygen	270.2	3329	1.3	105.6	52.3
Koppers-Totzek oxygen	285.0	3578	0.7	97.6	50.4
Wellman-Galusha air	159.4	2948	0.5	136.4	54.6
Winkler air	116.3	2579	0.6	109.6	74.7

Table 1. SYNPOSIS OF FURNACE OPERATING CONDITIONS AND TEST RESULTS FOR A 45-DEGREE VANE ANGLE (Part 2)

Fuel	Gross heat input, Btu/hr	Flue products, %				Vol of flue products, CFH at 60°F	SCF air / SCF fuel	SCF flue products / SCF fuel
		N_2	CO_2	H_2O	O_2			
Natural gas	2,371,265	72.5	8.3	16.7	2.5	27,357	11.23	12.26
Lurgi oxygen	2,356,066	62.9	16.8	17.8	2.5	27,565	2.71	3.41
Winkler oxygen	2,350,940	63.1	18.3	16.1	2.5	26,169	2.43	3.06
Koppers-Totzek oxygen	2,348,367	65.0	20.2	12.2	2.6	24,356	2.51	3.07
Wellman-Galusha air	2,358,036	72.3	15.8	9.2	2.7	32,772	1.54	2.33
Winkler air	2,358,940	74.5	14.6	8.2	2.8	38,339	1.13	1.96

Table 1. SYNPOSIS OF FURNACE OPERATING CONDITIONS AND TEST RESULTS FOR A 45-DEGREE VANE ANGLE (Part 3)

Fuel	Flue-gas temp, °F	Rear-wall temp, °F	Emissivity		Flue NO, ppm
			Calc	Meas	
Natural gas	2553	2309	0.159	0.177	65
Lurgi oxygen	2442	2300	0.194	0.185	32
Winkler oxygen	2523	2309	0.189	0.218	73
Koppers-Totzek oxygen	2554	2327	0.174	0.190	104
Wellman-Galusha air	2434	2066	0.154	0.190	15
Winkler air	2335	2012	0.150	0.170	4

Table 2. SPECIES CONCENTRATIONS, ADIABATIC FLAME TEMPERATURES, AND GROSS HEATING VALUE (Wet) FOR MEDIUM- AND LOW-Btu GASES TESTED

Fuel	Temp, °F	CO	H_2	CO_2	CH_4	N_2	H_2O	Adiabatic flame temp, °F	Heating value, Btu/SCF
		vol %							
Koppers-Totzek oxygen	90	52.9	34.5	9.2	0.5	1.0	1.9	3578	284
	1200	49.0	31.7	8.6	0.5	0.9	9.3	3677	266
Winkler oxygen	90	32.9	41.2	20.0	3.0	1.0	1.9	3327	269
	1200	25.7	32.2	15.8	2.4	0.8	23.1	3371	212
Wellman-Galusha air	90	27.9	14.9	3.2	2.7	49.6	1.9	2948	166
	1200	26.2	14.0	3.0	2.5	46.5	8.0	3119	156

SUMMARY

All of the experimental results presented in this report were taken from a pilot-scale furnace fired with a movable-vane boiler burner (MVBB) at a heat input of 2.25 million Btu/hr.* In addition to natural gas, three low-Btu gases were tested: Winkler oxygen, Koppers-Totzek oxygen, and Wellman-Galusha air. The combustion air was preheated to 325°F and was varied with test fuel gases to give 3% oxygen (dry) in the flue.

Based on a detailed analysis of the experimental data, the following conclusions were made:

1. No concentration levels for the ambient and preheated low-Btu gases tested were ordered by adiabatic flame temperature.

2. Of the fuel gases tested, only 800°F preheat Winkler oxygen gas with 15% FGR and ambient Wellman-Galusha air had NO emission levels projected to conform with the New Source Performance Standard of 168 ppm (0.2 lb/10^6 Btu) for gas-fired boilers.

3. The NO emission data yielded an activation energy of 195.2 kcal/mole. These data also revealed a rate controlling reaction temperature that provides an empirical method of predicting NO emission levels for a variety of operating conditions including fuel preheat, air preheat, and external flue-gas recirculation.

4. An iterative calculation technique using a non-well stirred reactor model predicted furnace efficiencies for each test fuel in good agreement with the experimental results.

---

* It is EPA policy to use metric units. However, in this report, English units are occasionally used for convenience. See conversion table at the back of this volume.

DESCRIPTION OF TEST FACILITY

GAS GENERATING SYSTEM

The low-Btu gases tested during this program were produced using the gas generating and fuel preparation facility shown schematically in Figure 1. The critical item in the gas supply system is the reformer, pictured in Figure 2. This is a special gas generator that produces varying ratios of H_2/CO. Natural gas and carbon dioxide are fed to the reformer through a specially designed mixing tee. Additionally, steam may also be mixed depending on the desired H_2/CO ratio. The resulting mixture is supplied to four reaction retorts contained in a vertical cylindrical furnace, where the endothermic chemical reaction is completed at a temperature of 2100°F. Globally, the reaction scheme is the water-gas shift. The gas generated within the reaction tubes passes through water-jacketed coolers, where it is quenched to prevent deterioration of the H_2/CO ratio.

The reformed gas is compressed to 30 psig and pushed through an MEA (methyl-ethyl-amine)-CO_2, absorbing tower. This tower is used to remove CO_2 from the reformed gas if its concentration is above what is needed to to synthesize the desired low-Btu gas. The reformed gas then enters a mixing chamber, where it is blended with nitrogen, carbon dioxide, steam, and natural gas to reach the desired mixture of gas to be modeled. The synthesized gas is then fed to the fuel preheat furnace.

This preheat furnace has dimensions 3 feet x 4 feet x 4-1/2 feet. The 9-inch-thick furnace walls are made of firebrick enclosed by 2-inch insulating board and a 1/4-inch steel plate shell. This fuel preheater is mounted on 6-inch-diameter wheels, which ride in a steel channel, allowing the distance between the fuel preheater and pilot scale furnace to be varied. This variation is accomplished through a pulley system and a 2-hp reversible electric motor.

Six inspirating burners (each of 200,000 Btu/hr) fire the preheater. A W-shaped fuel preheater pipe made of 2-inch-diameter, 304 stainless steel pipe is inserted into the preheater. This preheat pipe is fixed to the fuel injection nozzle. The amount of fuel preheat pipe contained in the preheater can be varied by changing the preheat furnace position relative to the pilot-scale test furnace. Given in Table 3 are the gas types tested and the length of pipe in feet that must be inserted into the preheater with 2000°F walls to achieve the indicated preheat

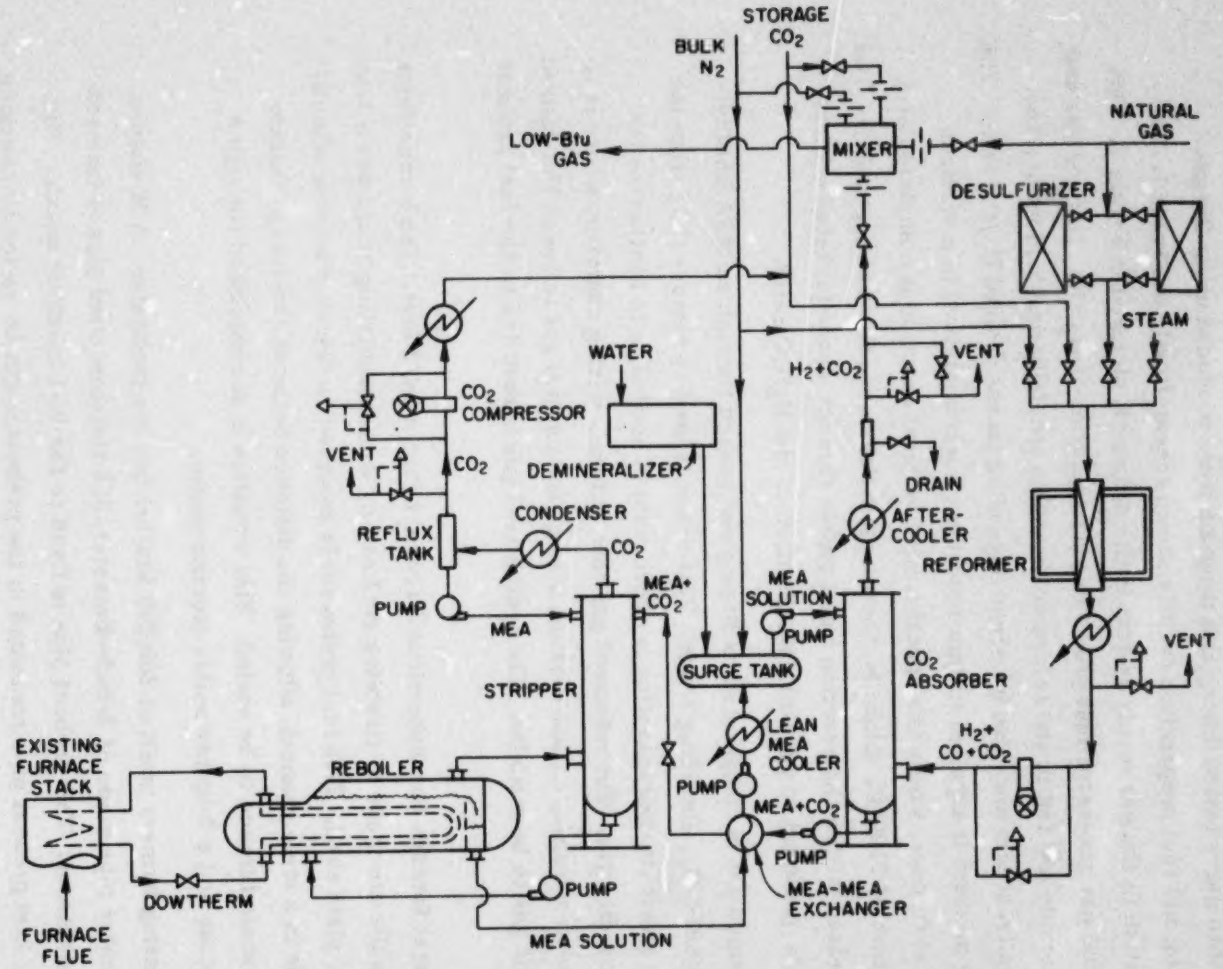

Figure 1. Schematic diagram of IGT gas-generating system

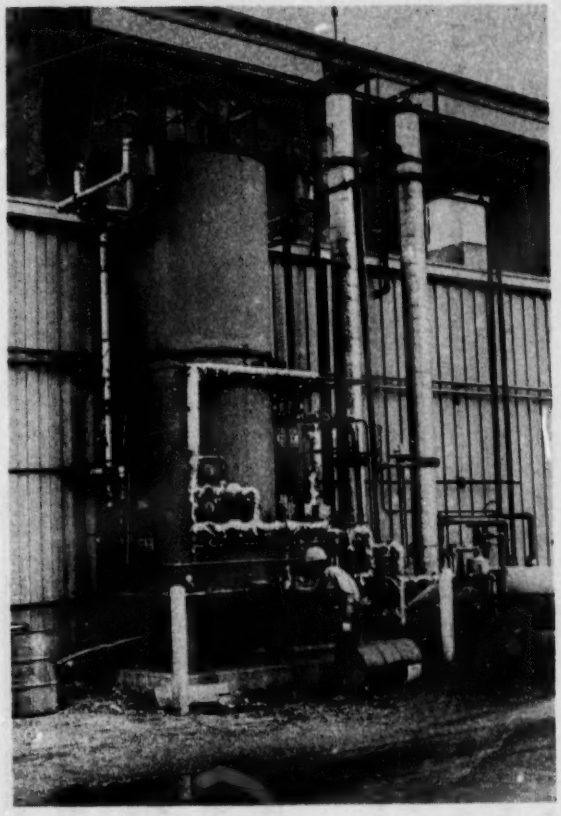

2a. Natural gas reforming system

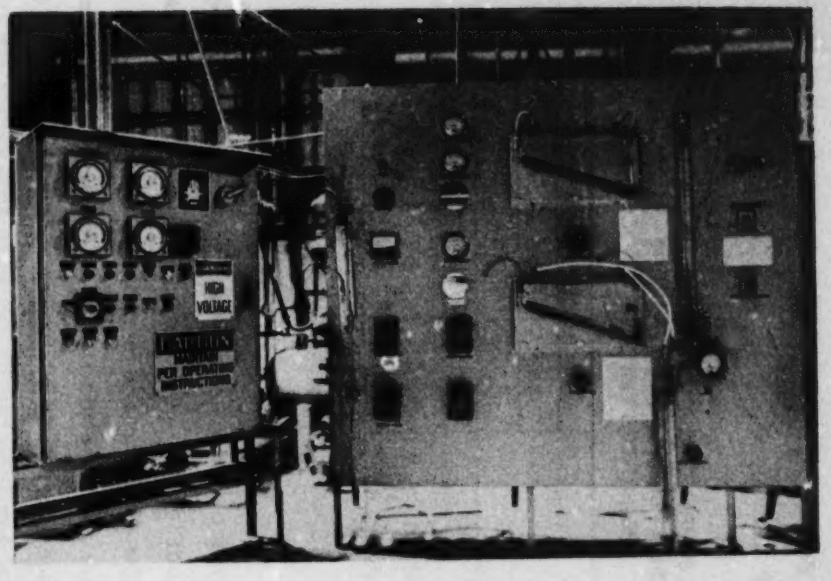

2b. Reformer controls and synthetic gas mixing panel

Figure 2. Gas-generating system

temperatures. After preheating, these synthesized gases are fed to the pilot-scale furnace for combustion testing.

Table 3. PREHEATER TUBE LENGTHS VERSUS PERHEAT TEMPERATURE FOR GASES TESTED

	Preheat temperature, °F		
	400	800	1200
	ft		
Winkler oxygen	4	8	15
Koppers-Totzek oxygen	2.8	6.2	11.4
Wellman-Galusha air	4.8	10.8	20

PILOT-SCALE FURNACE

The experimental work was conducted on a rectangular furnace with a 25-sq-ft cross-sectional area and a 13-foot length. This furnace can be end- or sidewall-fired at a rate of 4 million Btu/hr. The furnace is equipped for in-the-flame sampling, preheated air, and flue-gas recirculation. (See Figure 3.) This furnace is capable of operating at temperatures up to 3000°F or as low as 1600°F at a constant (maximum) gas input of 4 million Btu/hr and up to 40% excess air. Cooling is achieved with cooling coils embedded in the refractory walls. The furnace is constructed completely of 9-inch-thick cast refractories, with removable panels in one sidewall to permit insertion of sampling probes (Figure 4.) The overall furnace system is shown schematically in Figure 5. The system is flexible enough that the following operating parameters can be independently varied:

- Heat input, to 4 million Btu/hr (8.0 million for certain burners)
- Air input, to 40% excess
- Heat losses, to the furnace walls by changing flow in water-cooling tubes cast into the refractories
- Combustion air temperature, to 1000°F
- Flue-gas recirculation capability, to 35% of combustion air
- Furnace pressure, to +0.05 inch of water.

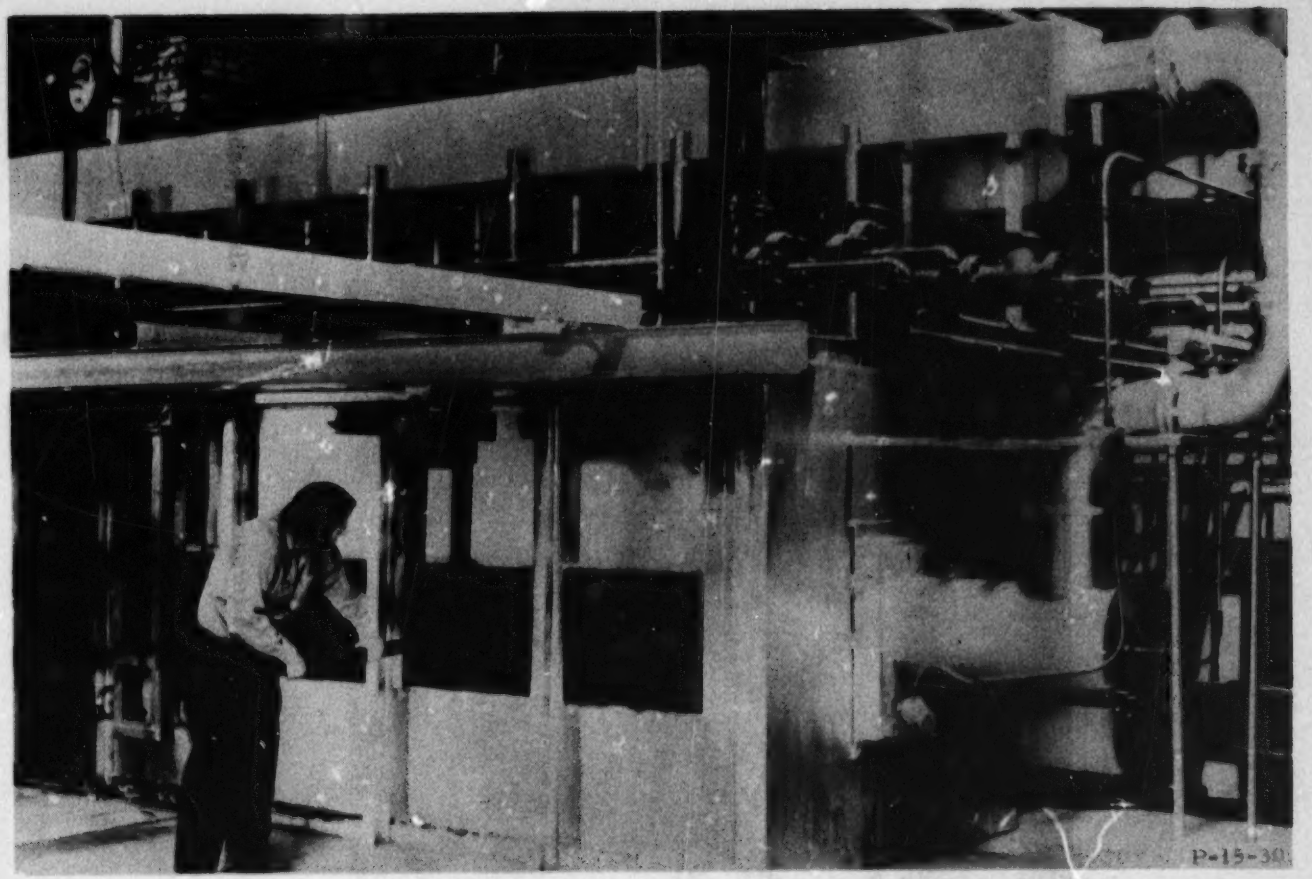

Figure 3. Rectangular test furnace

Figure 4. Removable sidewall furnace panels for interior flame probing

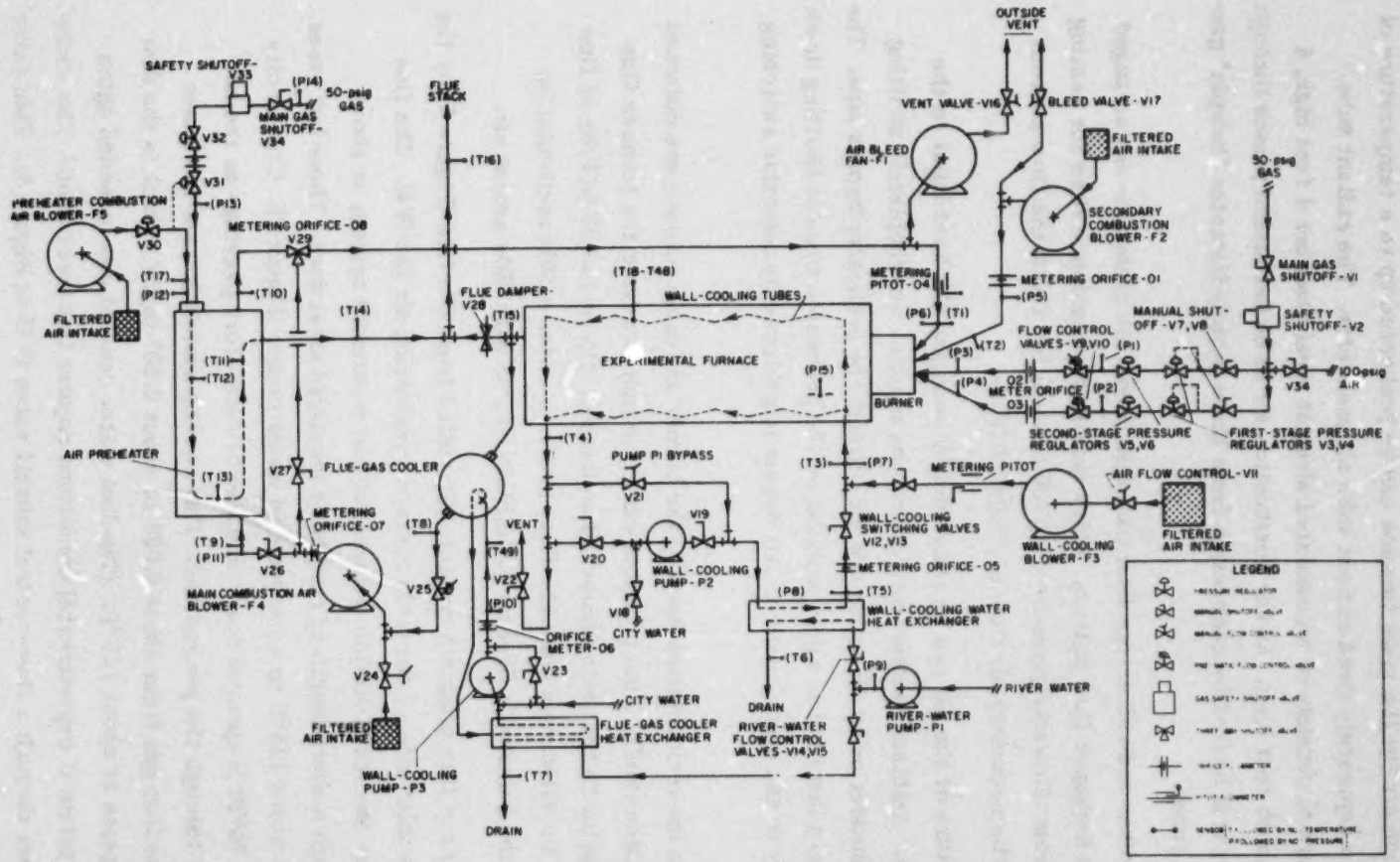

Figure 5. Overall system schematic design of rectangular test furnace

The combustion air for the main furnace can be preheated up to a temperature of 1000°F with a separately fired radiant tube air preheater. The radiant tube furnace (Figure 6) consists of an insulated airtight steel chamber 4 feet high, 4 feet wide, and 16 feet long. As the combustion air to be preheated passes through this chamber, it is heated by convection from three 6-inch-diameter "hairpin" gas-fired radiant tubes.

The radiant tubes and refractory flow passages inside the preheater are arranged to provide an S-shaped flow pattern, which maximizes residence time for heating at the maximum allowable pressure drop (20 ounces) for which the flow pattern will provide the necessary air flow of 75,000 SCF/hr.

The temperature of the air can be regulated by changing the heat input to the radiant tubes. Ambient temperature air can be supplied by completely shutting down the preheater or by directing the air through the preheater bypass pipe. The bypass pipe was installed to allow working on the preheater without shutting down the air supply to the main furnace. Air bypass is achieved by selective switching of valves.

Flue products for recirculation back to the burner and main furnace are obtained from the furnace itself. Flue products can be withdrawn from the furnace flue passage just prior to the main furnace flue damper. Up to 14,000 SCF/hr of flue products can be withdrawn from the flue, which provides a 30% recirculation factor when the furnace is fired at 3.5 million Btu/hr with 20% excess air.

The main furnace flue products are actually pulled from the flue (Figure 5) by the suction in the inlet side of the main furnace combustion air fan (F4). The flue products enter the recirculation withdrawal and treatment system at about 2800°F through a short length of internally insulated steel duct. These hot gases are cooled to about 125°F in a packed-bed water cooler (Figure 7). Cooled city water (about 70°F) is sprayed down on a bed of refractory packings as the hot gases pass up through the packed bed. This cooling system lowers the water content of the flue gas from about 0.008 to about 0.007 lb/CF, which is the dew point of the gases at about 125°F. (The lost water content can be added again later in the system if experimental conditions require this treatment.) The cooled gases then pass through a flow-control shutoff valve (V25 in Figure 5). This valve controls the flue-gas flow rate, which regulates the percentage of recirculated products. This valve is interlocked to an outlet temperature sensor on the gas

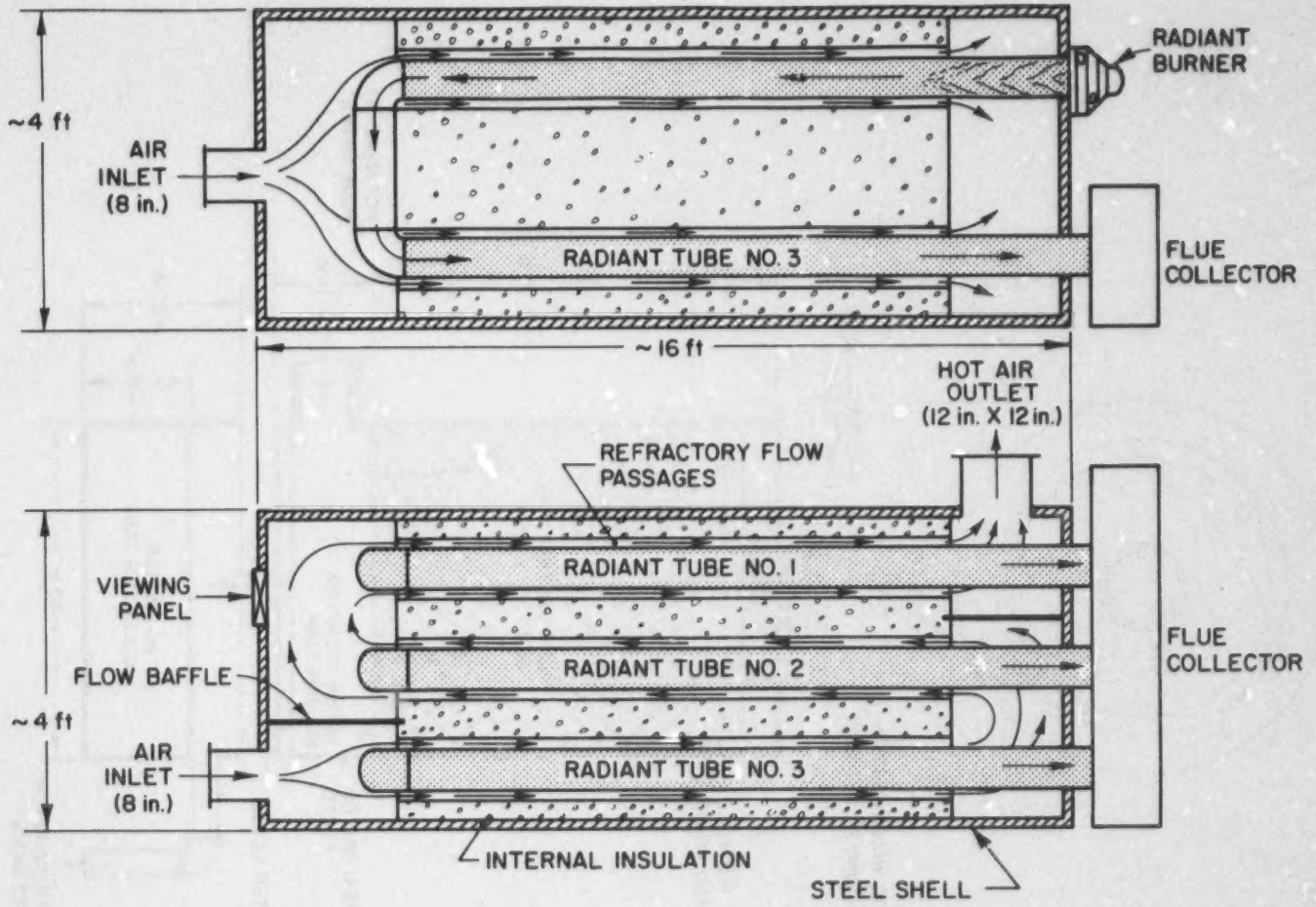

Figure 6. Radiant tube preheater for main furnace combustion air

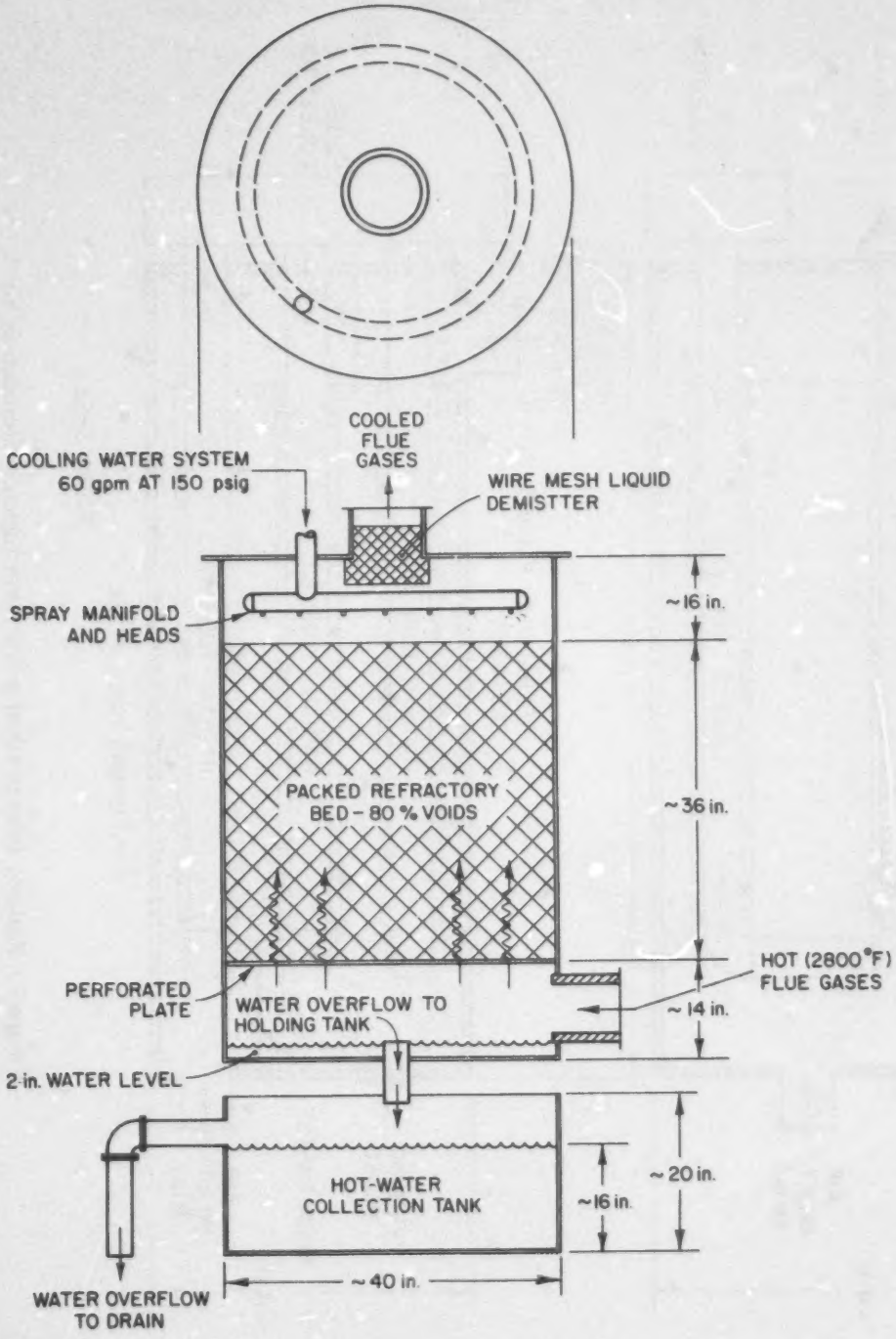

Figure 7. Flue-gas cooler

cooler. If the outlet temperature of the gases exceeds 150°F, which would damage the combustion air fan, the control valve (V25) shuts down. This stops the flow of flue gases. Beyond the flue-gas control valve, the flue gases are mixed with the required amount of air for combustion. A control valve (V24) regulates the amount of air pulled in by the fan. The total amount of air for combustion and flue products is metered with an orifice plate (O7) at the outlet of the fan. The flue products and air then pass into the air preheater or preheater bypass pipe.

The water used in the flue-gas cooler is clean city water, which is continuously recycled. A water flow of 60 gpm is supplied at 150 psig by a turbine pump to a series of spray heads in the gas cooler. The hot (200°F) spent water flows out of the cooler into an atmospheric holding tank. This tank is equipped with a constant-level overflow to the building drain. In this way, any condensed water from the combustion is removed and disposed of in the sewer. The water in the holding tank is periodically treated with sodium hydroxide to prevent acid buildup in the water due to condensing flue-gas components. One such component removed by the flue-gas cooler is NO_2. The hot water from the water holding tank is cycled through an American Standard heat exchanger capable of removing 1.5 million Btu/hr of heat from the water. Cooling in the heat exchanger is provided by a flow of river water at a rate of about 150 gpm at 80 psig. The river water is supplied by a river adjacent to the test facility through a service pump (P1) maintained by IGT.

ANALYTICAL TEST EQUIPMENT

Figure 8 is an overall view of furnace controls and the analytical instrumentation package. The equipment used for concentration measurements of chemical species during this progam is listed below; these analyzers included the following items:

1. Beckman 742 Polarographic Oxygen (O_2)
2. Beckman Paramagnetic Oxygen (O_2)
3. Beckman NDIR Methane (CH_4)
4. Beckman NDIR Carbon Monoxide (CO)
5. Beckman NDIR Carbon Dioxide (CO_2)
6. Varian 1200 Flame Ionization Chromatograph (Total HC and C_2 to C_9)

Figure 8. Control room facility and analytical instrumentation

7. Beckman NDIR Nitric Oxide (NO)

8. Beckman UV-NO_2

9. Hewlett-Packard Thermoconductivity Chromatography, Hydrogen (H_2), Nitrogen (N_2), Argon (A_2), CO, CO_2, C_1 to C_5, Oxygen (O_2)

10. Beckman Chemiluminescent NO-NO_2

11. Data Integration System.

This instrumentation package allowed concentration measurements of the following major components: 1) measurement of hydrocarbon compounds C_1 to C_9; 2) independent check of NO-NO_2 chemiluminescent with NDIR-NO and NDUV-NO_2; 3) independent check of paramagnetic O_2, polarographic O_2, NDIR-CH_4, NDIR-CO, and NDIR-CO_2 with the respective chromatographic species concentrations; and 4) measurement of hydrogen (H_2), argon (A_2), and nitrogen (N_2).

The following sections give a general description of the measurement system used for this program.

NO AND NO_2 INSTRUMENTATION

The chemiluminescent NO_x and NDUV-NO_2 system was mounted in a roll-around cabinet that could be placed out at the furnace. This was important in minimizing sampling distances, which can affect accuracy. The chemiluminescent unit was equipped with a carbon converter. Test work by IGT and others has demonstrated that in a reducing environment the carbon converter maintains a better conversion efficiency than converters made of stainless steel, quartz, or molybdenum.

The instrumentation was calibrated by using both a permeation tube with a controlled known release of NO_x and certified prepared cylinders of NO and NO_2 gases.

The sample gas was drawn from the furnace through a special alumina probe by a Dia-Pump Model 08-800-73 all stainless-steel and Teflon® pump delivering approximately 0.4 CF/min. (This sample delivery rate was dictated by the requirements of the measuring instruments.) The sample is immediately passed through a stainless-steel large-particle filter. Both the pump and filter were kept above 100°C to prevent condensation of the water vapor inherent to combustion products.

CO, CH_4, AND CO_2 MEASUREMENTS

Nondispersive infrared analyzers were used for carbon monoxide, methane, and carbon dioxide measurements. These analyzers do not affect the sample gas and can be operated in series. They were calibrated by using certified gases with known concentrations of the species being determined. The infrared analyzers require a completely dry sample. Therefore, the sample was first passed through a water trap and a 3 A molecular drying sieve. A small in-line filter was placed immediately after the drying tube to trap particles of sieve that may be carried over by the gas stream.

OXYGEN MEASUREMENTS

A portion of the "conditioned" sample gas is diverted from the NDIR units to a Beckman Model 600 paramagnetic analyzer. A second oxygen analyzer, a Beckman Model 742 polarographic, was used as a cross-check on the oxygen concentration. The Model 742 analyzer has an advantage over the paramagnetic in time response.

CHROMATOGRAPHIC MEASUREMENTS

As a detailed gas analysis was required, the sample was fed to a Hewlett-Packard 7620-A thermal conductivity chromatograph, which permitted concentration evaluations of hydrogen, nitrogen, argon, oxygen, carbon monoxide, carbon dioxide, and hydrocarbons C_1 to C_5. To achieve separation of these species, a helium carrier gas was used in conjunction with a Porapak Q column. Three temperature program rates were also required, ranging from -100° to $300^{\circ}C$. A sample loop volume of 100 ml was used to ensure linearity in the hydrogen response for concentrations up to 60%.

For total hydrocarbon analysis, a Beckman hydrocarbon analyzer was used. A detailed hydrocarbon analysis could be made using a Varian 1200 flame-ionization chromatograph. All chromatographic readings were electronically integrated and printed out as a function of resolution time.

In addition to flue-gas analysis, a major task of this program was to map profiles of temperature, chemical species, and flame emissivity. Modified designs of the International Flame Research Foundation (IFRF) were used to construct probes, which enabled this type of data collection.

Figure 9 shows the assembly drawing of the gas-sampling probe used in both the flame and the flue. To minimize NO_2 reduction in the probe, an alumina tube was inserted for the first 18 inches and was joined to Teflon tubing to carry the gas sample to the analyzers.

Temperature data were collected using a suction pyrometer; the design is illustrated in Figure 10. A Pt-Pt Rh 10% thermocouple was used. The efficiency of the pyrometer was measured at 96% with a 25-second response time.

The gas-sampling probe, suction pyrometer, and radiation cooling target were all designed to be installed in the general probe holder shown in Figure 11.

To evaluate radiation intensity, which is needed for a determination of flame emissivity, a PR 200 Pyroeletric Radiometer, manufactured by Molectron Corp. in Sunnyvale, California, was used. Figure 12 shows the pyroelectric radiometer plus radiation shield. This radiometer uses a permanently poled lithium tantalate detector that is capable of resolving radiant power into the nanowatt range while maintaining a continuous spectral response from the vacuum UV to 500 μ m. A built-in optical calibration system in the form of a highly stable LED (light-emitting diode) that is calibrated against an NBS traceable standard of total irradiance permits a direct correlation of experimental data from different trials.

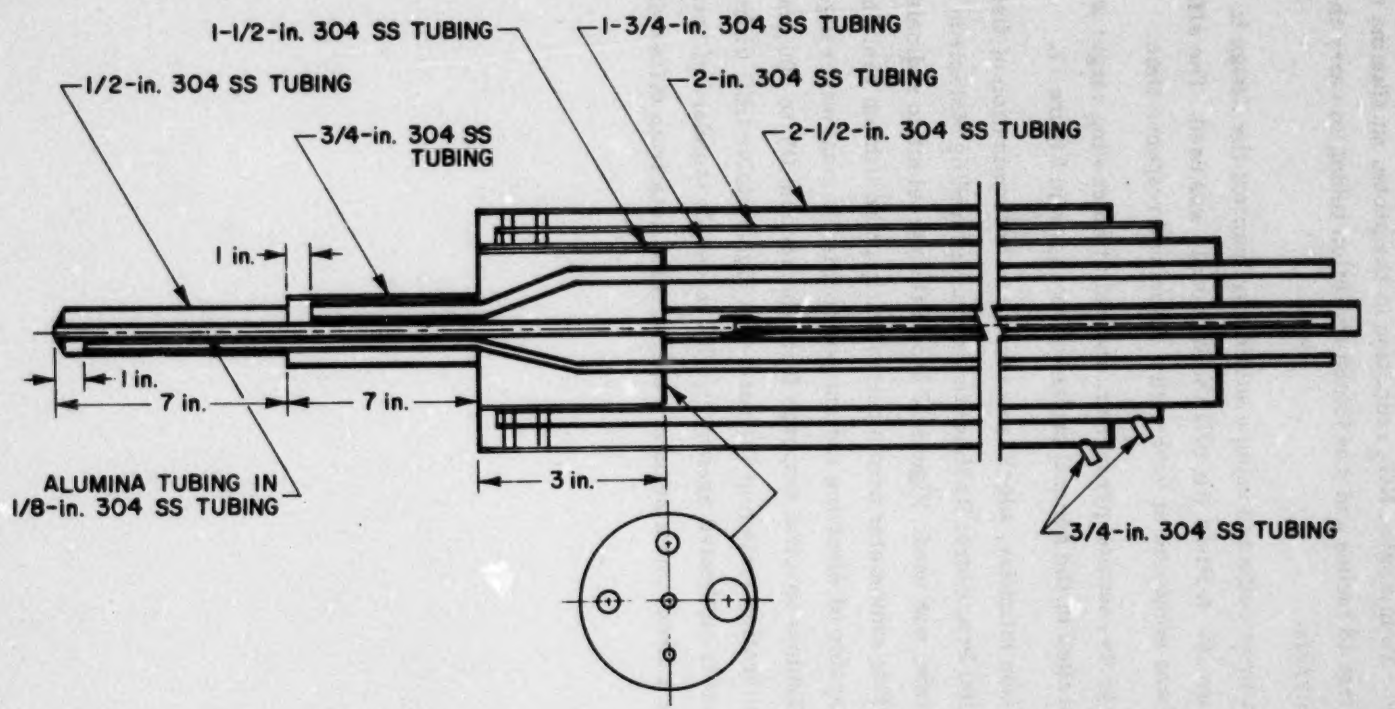

Figure 9. Gas sampling probe head for nonparticulate flue gases

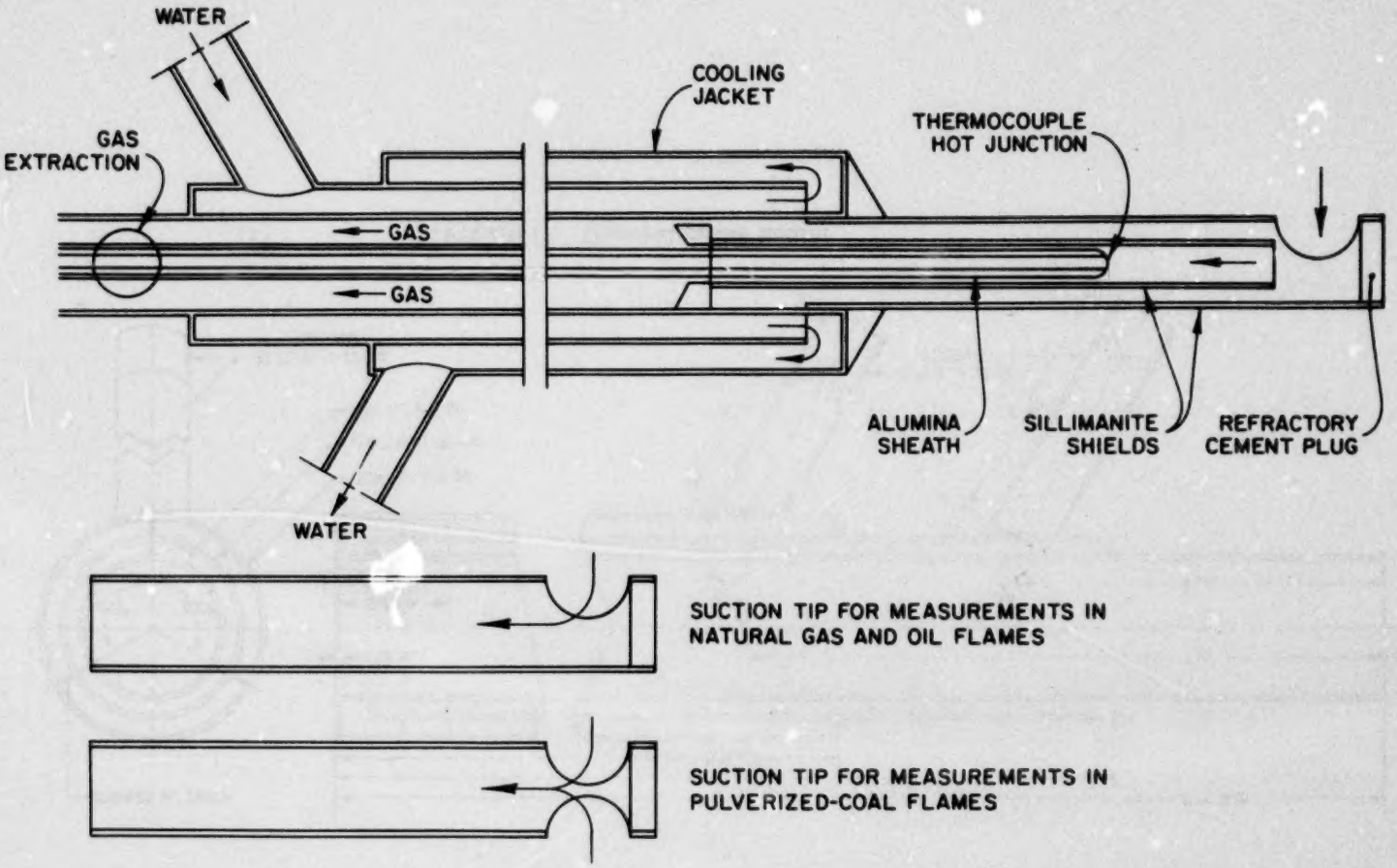

Figure 10. Modified IFRF temperature probe

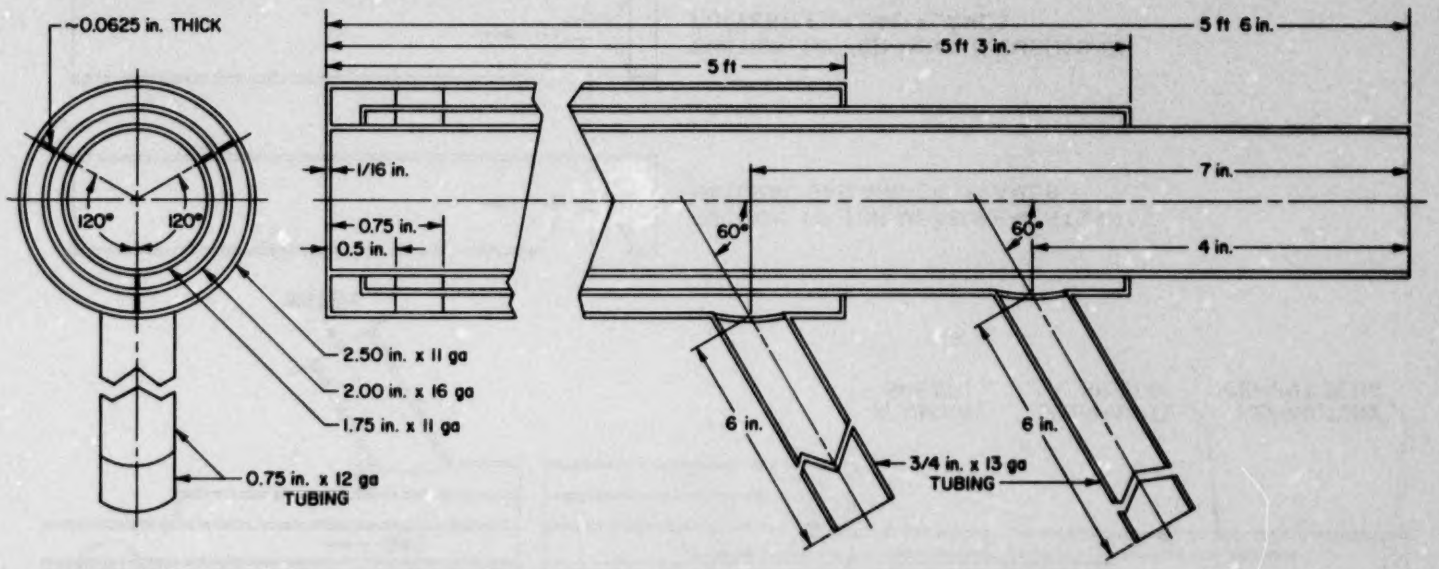

Figure 11. General probe holder

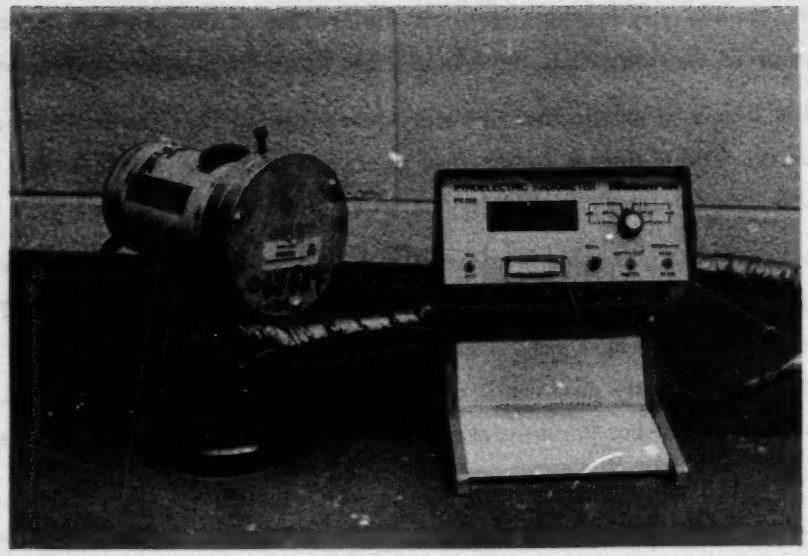

Figure 12. Pyroelectric radiometer (used for emissivity measurements)

EXPERIMENTAL PLAN

All test data were collected using a single register movable-vane boiler burner (MVBB) with an axial fuel injector. An assembly drawing of the MVBB tested is shown in Figure 13. The combustion air enters perpendicular to the axes of the burner and passes through a register of guide vanes that impart a degree of spin to the air, dependent on the vane orientation.

Figure 14 illustrates how the angle of the movable vane is measured. The ratio of the average tangential and radial velocity components at the exit of the movable-vane register depends only on the geometric dimensions of the vanes in the axis perpendicular cross section (assuming a negligible Reynolds number influence).

A straight pipe was used as the fuel injector, guaranteeing that the fuel had only an axial velocity. The diameter of the fuel injector was varied for fuel type to maintain an injection velocity of 100 ft/s at 70°F.

The burner block used during this program had a 30-degree divergent angle with a 15.2-cm (diameter) entrance and a 48.2-cm (diameter) exit to the furnace. To maximize flame stability the throat nozzle position was used through this program. The throat nozzle position is located 2.5 cm from the burner block entrance within the 15.2-cm (diameter) refractory duct connecting the burner with the block.

Burner operating conditions used throughout the program had the level of flue oxygen fixed at 3% (dry) with the combustion air preheated to 325°F (unless specified differently). These conditions are considered typical for utility boiler burners.

Based on the overall program objective of evaluating changes in boiler performance and NO emisson levels when retrofitting from natural gas to "high-temperature" low-Btu gas, it was necessary to select an operating variable to model the pilot-scale test furnace against a field service boiler. Several parameters were considered, including operating wall temperature, heat absorption profile, and firing density. It was decided to match the temperature of the combustion products from natural gas at the pilot-scale furnace exit to the temperature measured between the boiler and the secondary superheater section

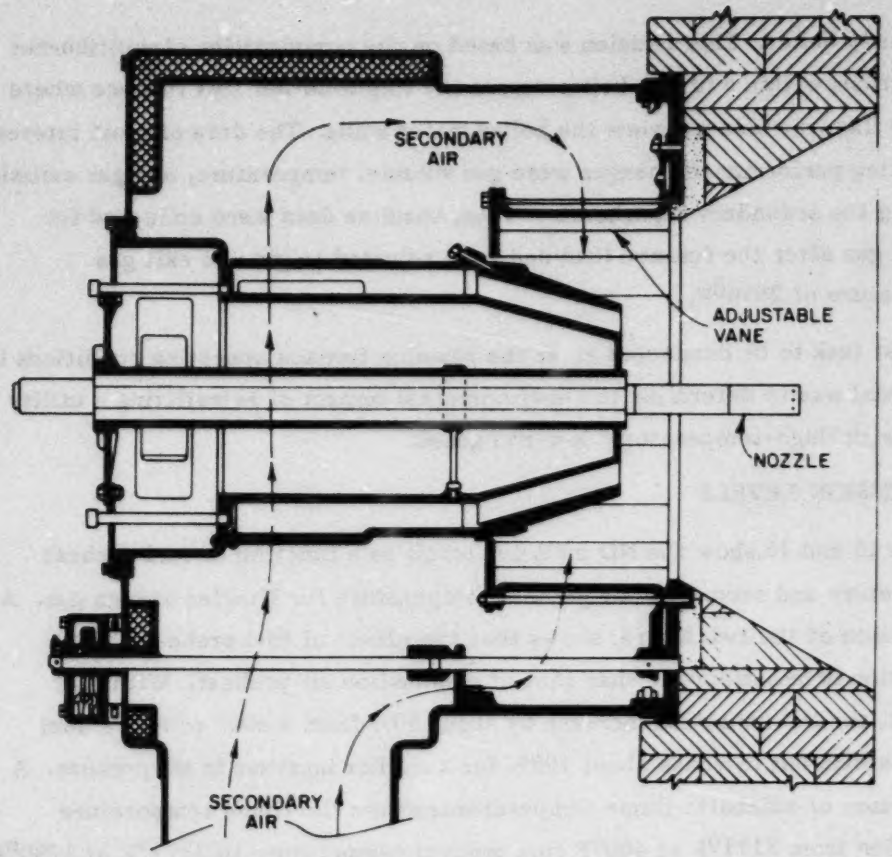

Figure 13. Diagram of movable-vane boiler burner

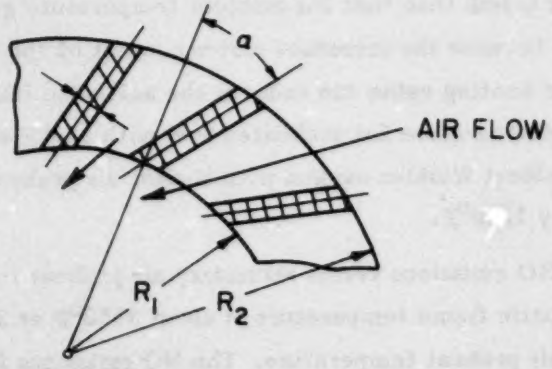

Figure 14. Method of measuring movable-vane angle for boiler burner

of a utility boiler. This decision was based on the complexities of multiburner interactions within a utility boiler versus the single-burner test furnace where several flames would not view the boiler water walls. The data of most interest in evaluating performance changes were gas volume, temperature, and gas emissivity entering the secondary superheater. Thus, baseline data were collected for natural gas after the furnace load had been adjusted to give an exit gas temperature of 2550°F.

The first task to be conducted after the baseline furnace operating conditions had been fixed was to determine the environmental impact of retrofitting a utility boiler with "high-temperature" low-Btu gases.

NO EMISSION LEVELS

Figures 15 and 16 show the NO emission levels as a function of fuel preheat temperature and secondary air preheat temperature for Winkler oxygen gas. A comparison of the two figures shows that the effect of fuel preheat on NO production is less dramatic than that of combustion air preheat. With fuel preheat, the NO emissions increase by about 50% from a 400° to 800°F fuel temperature, but increase about 100% for a similar increase in air preheat. A comparison of adiabatic flame temperatures shows the flame temperature increasing from 3171°F at 400°F fuel preheat temperature to 3371°F at 1200°F fuel preheat temperature. Correspondingly, the adiabatic flame temperature with air preheat increases from 3327°F at 325°F to 3562°F at 800°F secondary air preheat temperature. The level of emissions from preheated Winkler oxygen intermediate-Btu gas is less than that for ambient temperature gas at 325°F air preheat temperature because the increased water content of the hot gas (23% versus 2%) lowers the heating value and reduces the adiabatic flame temperature. The adiabatic flame temperature for preheated fuel with 325°F secondary air does not equal that for ambient Winkler oxygen with similar air preheat until a fuel temperature of nearly 1200°F.

Figure 17 shows the NO emissions versus secondary air preheat for natural gas. The natural gas adiabatic flame temperature is about 3680°F at 325°F and 3880°F at 800°F secondary air preheat temperature. The NO emissions follow a consistent trend, increasing as the adiabatic flame temperature rises.

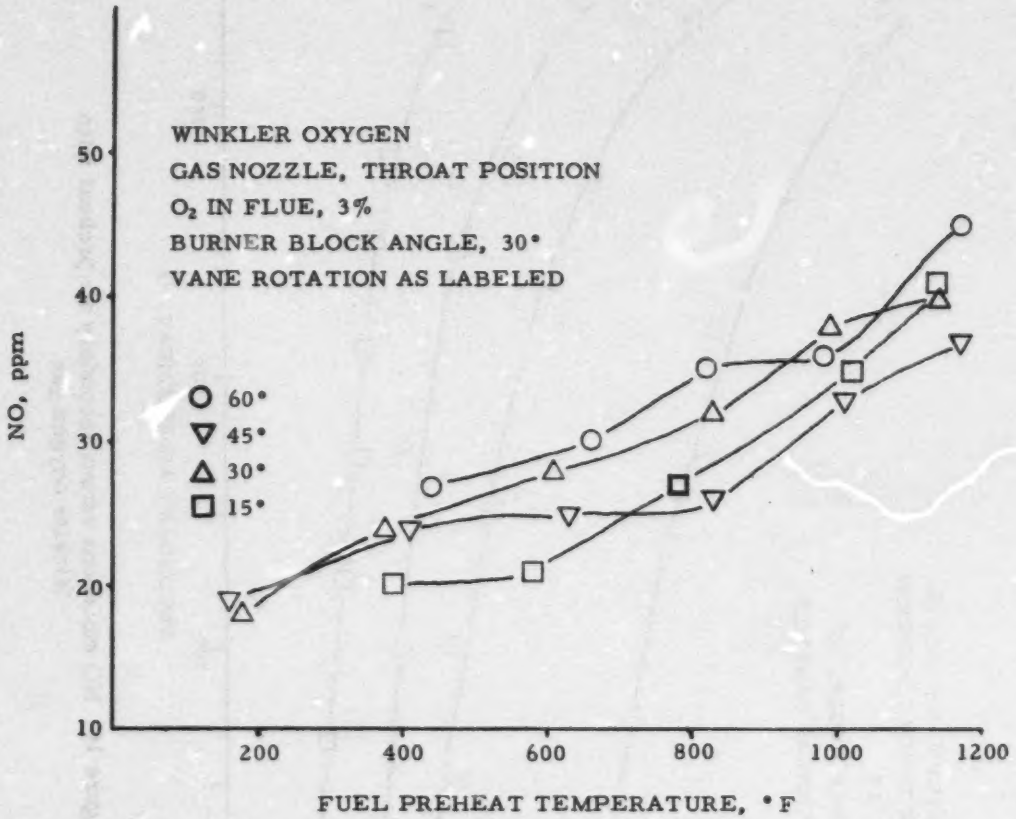

Figure 15. NO emissions versus fuel gas preheat with Winkler oxygen gas

Reproduced from best available copy.

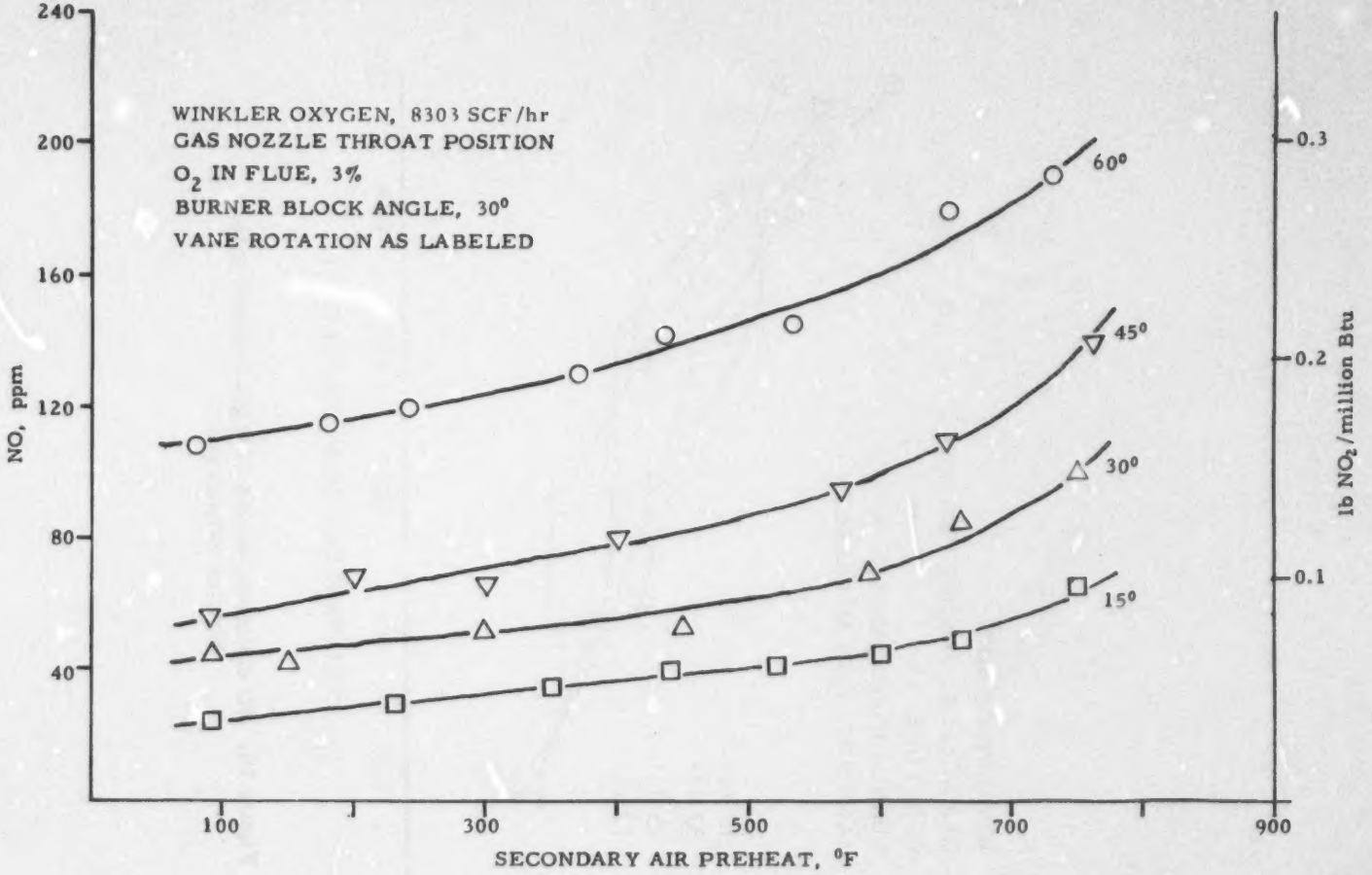

Figure 16. NO emissions versus secondary air preheat with Winkler oxygen gas

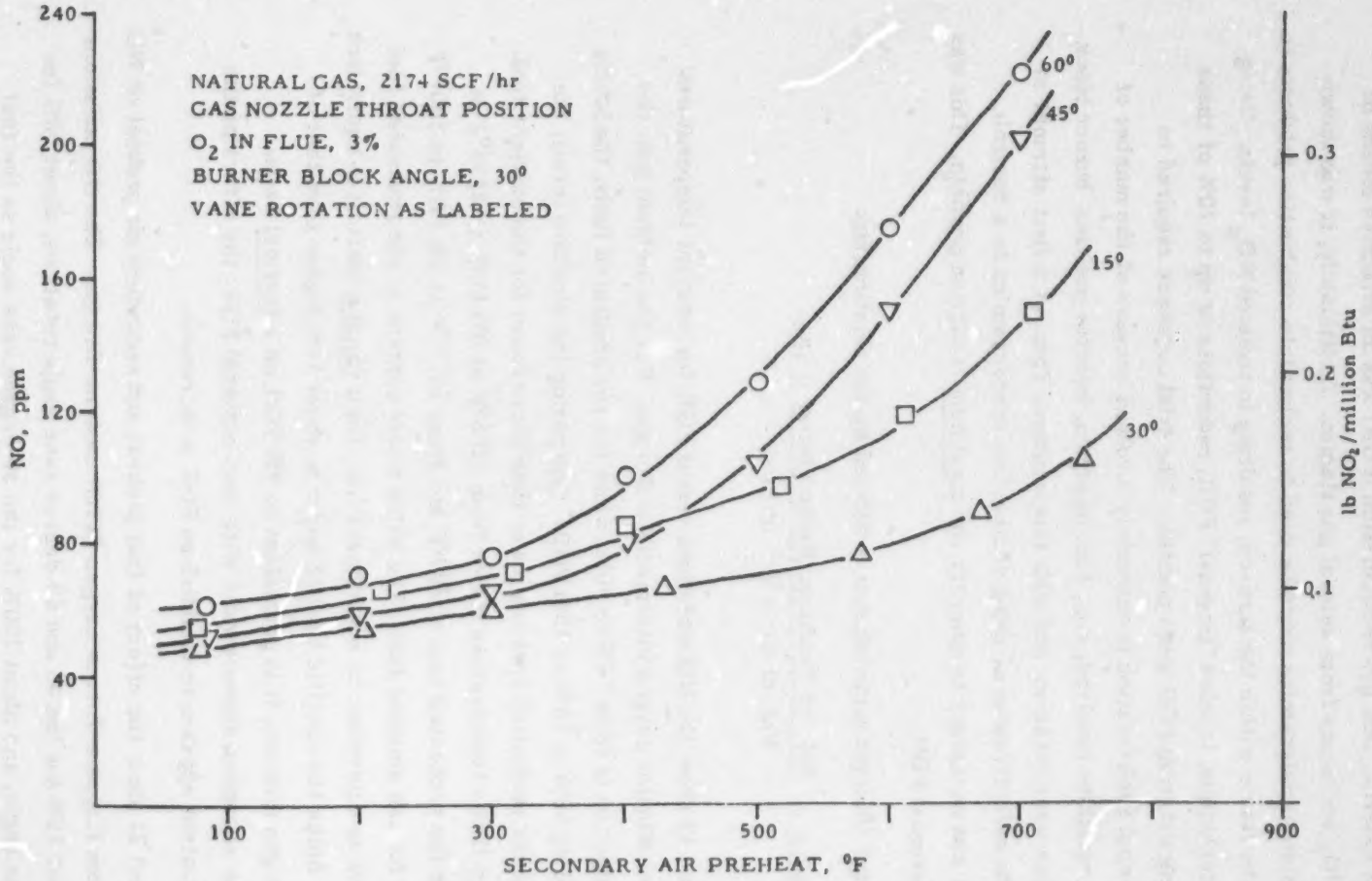

Figure 17. NO emissions versus secondary air preheat with natural gas

It was demonstrated during a prior phase of this program (EPA Report No. 600/2-76-098a) that external flue gas recirculation (FGR) was an effective means of controlling NO_x emissions from natural gas flames. Additionally, it was shown that combustion aerodynamics could be used to recirculate combustion products to the base of the flame within the furnace, resulting in reduced NO_x levels. Using this control technique, labeled "internal" FGR, reductions of up to 70% of those achieved using external FGR were possible. The trial sequence required to evaluate internal recirculation is extremely involved because of the number of independent variables involved, e.g., fuel injection, injector position, burner block angle, movable-vane rotation, and wall temperature. Thus, as a first attempt at evaluating the effectiveness of using combustion aerodynamics as a control technique, it was necessary to quantify the maximum reduction possible. This was done using external FGR.

The percentage flue-gas recirculation is defined by the relationship:

$$\% \text{ FGR} = \frac{\text{Vol of Products Recirculated}}{\text{Vol of Air + Vol of Fuel}} \times 100$$

Figures 18 and 19 show the NO emissions versus FGR for ambient temperatures and preheated Winkler oxygen intermediate-Btu gas. For the ambient gas, the emissions reduction is from 70% to 90%, while for the preheated fuels, the levels were reduced by 60% to 70% at 15% FGR. Comparing the absolute levels, the emissions for the preheated fuel are lower than those found for the ambient fuel. The adiabatic flame temperature varies from 3268°F at 0% FGR to 2933°F at 15% FGR for the preheated fuel at 800°F and from 3327°F at 0% FGR to 3007°F at 15% FGR for the ambient fuel. The extra water content of the preheated fuel can be viewed as equivalent to additional FGR. On a volume basis, it is equivalent to 8% FGR. Since the specific heat of water is about 11% higher than that of CO_2/N_2 flue-gas mixture, it is equivalent to 9% FGR on a thermal basis. Although this argument appears valid with zero external FGR, the effect of the fuel water content appears to diminish as FGR is increased.

Figures 20 and 21 show the effect of fuel preheat and secondary air preheat on NO emissions from Koppers-Totzek oxygen (KTO) medium-Btu gas. The NO emissions increase about 15% for the 45 and 60-degree vane angle rotations, about 50% for the 15-degree angle, and about 100% for the 30-degree vane angle as the fuel

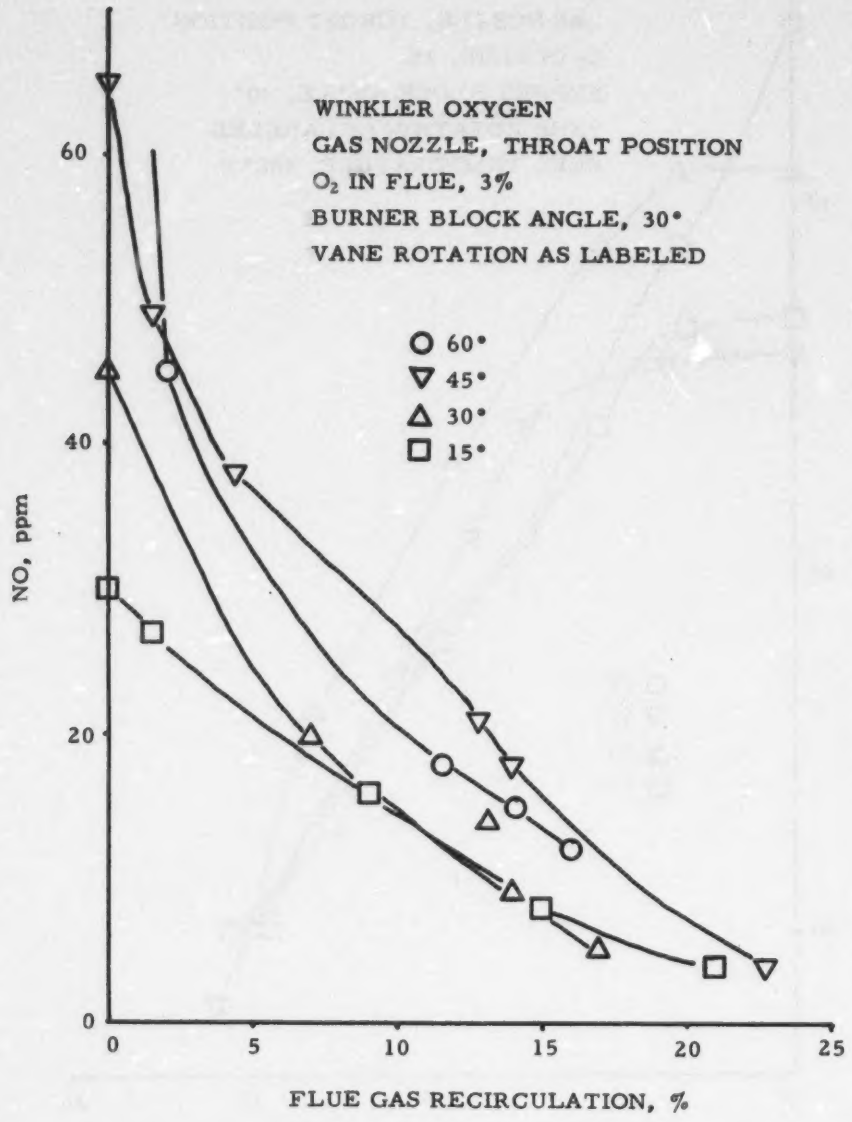

Figure 18. NO emissions versus FGR for "ambient" Winkler oxygen fuel

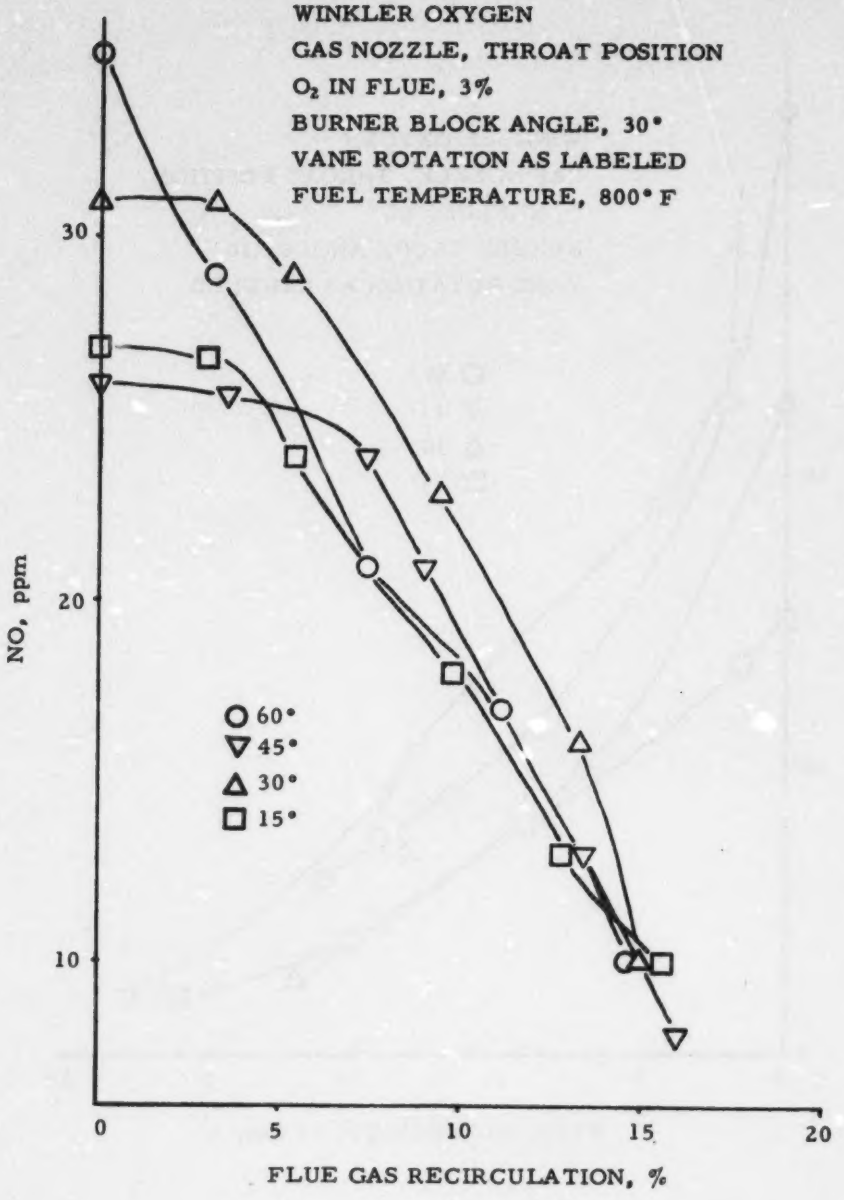

Figure 19. NO emissions versus FGR for Winkler oxygen preheated to 800°F

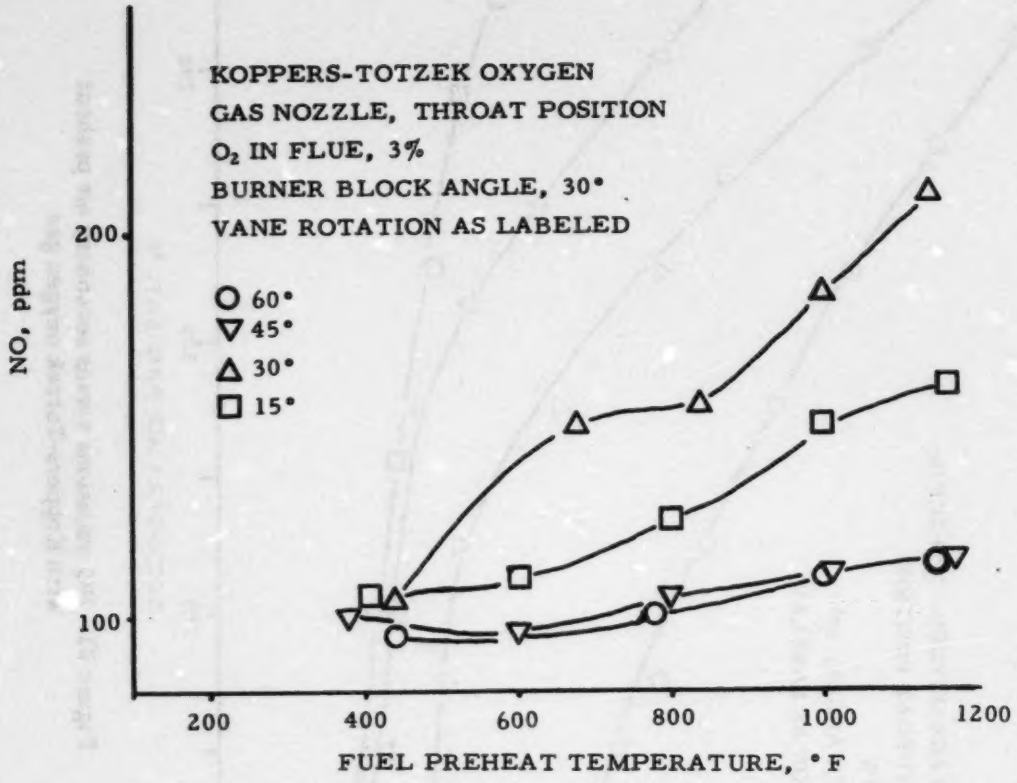

Figure 20. NO emissions versus fuel gas preheat with Koppers-Totzek oxygen gas

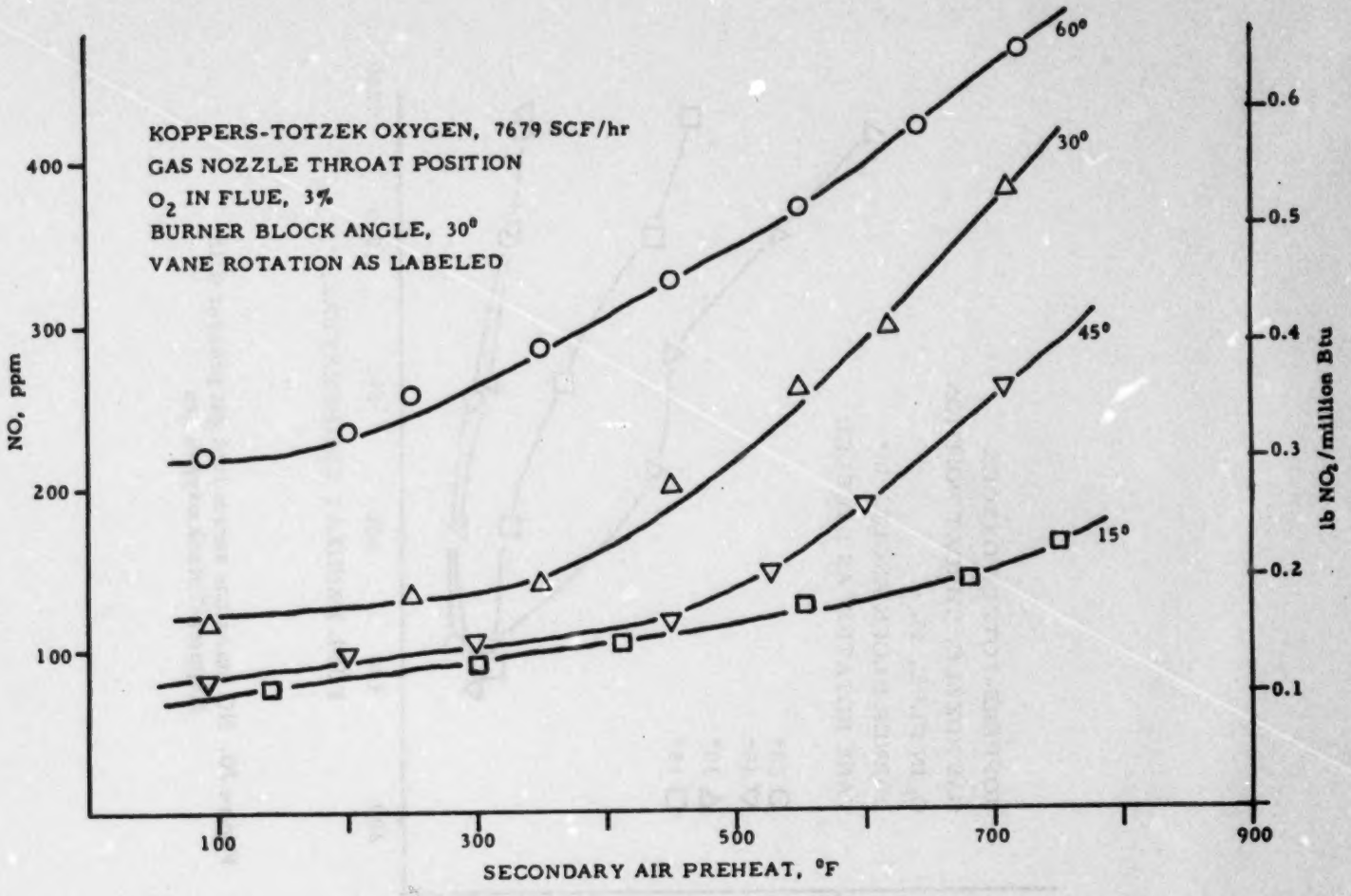

Figure 21. NO emissions versus secondary air preheat with Koppers-Totzek oxygen gas

preheat increases from 400° to 1200°F. These increases in emissions are less than the 200% to 300% increases seen for the air preheat trials. The only exception is the 50% emissions increase seen for the 15-degree angle during the air preheat trials. The adiabatic flame temperatures for preheated fuel vary from 3537°F at 400°F to 3667°F at 1200°F. With air preheat, the flame temperature increases from 3578°F at 325°F to 3745°F at 800°F. The adiabatic flame temperature for preheated fuel is high for KTO because the water content goes from only 1.9% to 9.3% comparing ambient with hot gas. A comparison of emissions with those previously seen for natural gas shows that they follow the trend suggested by the adiabatic flame temperatures, i.e., higher emissions with higher adiabatic flame temperature.

Figures 22 and 23 show the NO emissions versus FGR for ambient and preheated KTO intermediate-Btu gas. The emissions are reduced by 50% to 60% at 15% FGR for the ambient gas, which is comparable to the 60% to 65% reduction found in previous studies with natural gas. With fuel preheated to 800°F, the reduction in emissions is again 50% to 60% at 15% FGR except for the 45-degree vane angle data. In general, the emissions are higher than those seen for ambient KTO. The adiabatic flame temperature varies from 3578°F at 0% FGR to 3191°F at 15% FGR for ambient KTO and from 3605°F at 0% FGR to 3335°F at 15% FGR for KTO preheated to 800°F. These emissions data follow the trend of increased emissions with increased adiabatic flame temperature.

Figures 24 and 25 show the NO emissions from Wellman-Galusha air (WGA) low-Btu gas versus fuel preheat and secondary air preheat. Here the NO emissions double with a fuel preheat temperature increase from 400° to 1000°F. For a similar increase in secondary air preheat, the NO emissions double for the 45 to 60-degree vane angles and increase by 50% and 20% for the 30 and 15-degree angles, respectively. The adiabatic flame temperature varies from 2916°F at 400°F to 3119°F at 1200°F fuel gas preheat. With secondary air preheat, the flame temperatures go from 2948°F at 325°F to 3112°F at 800°F air preheat temperature. The absolute levels for the WGA low-Btu gas NO emissions are lower than those seen in Figure 17 for natural gas. Because of the low value of the WGA low-Btu gas NO emissions, no FGR trials were run with this fuel.

Figure 26 shows a plot of ln [NO] versus the reciprocal of the adiabatic flame temperature, T_{AF}. Included are data for the preheated fuels with and without

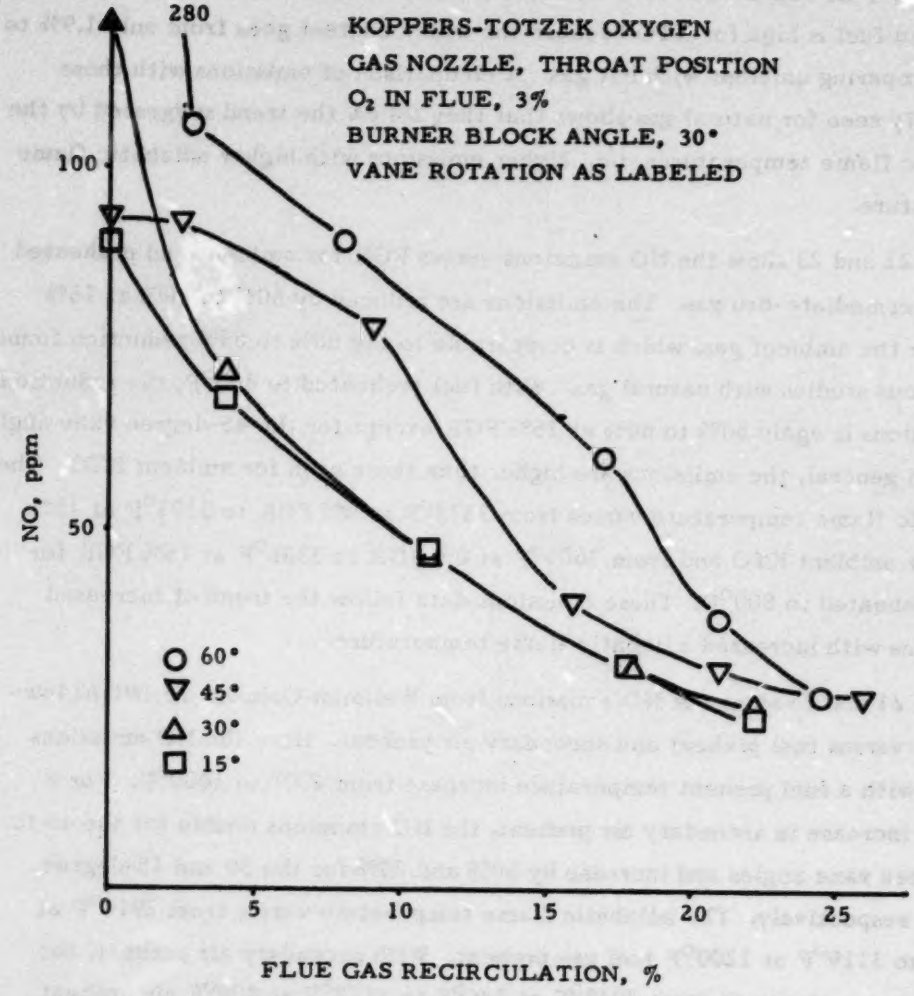

Figure 22. NO emissions versus FGR for "ambient" Koppers-Totzek oxygen fuel

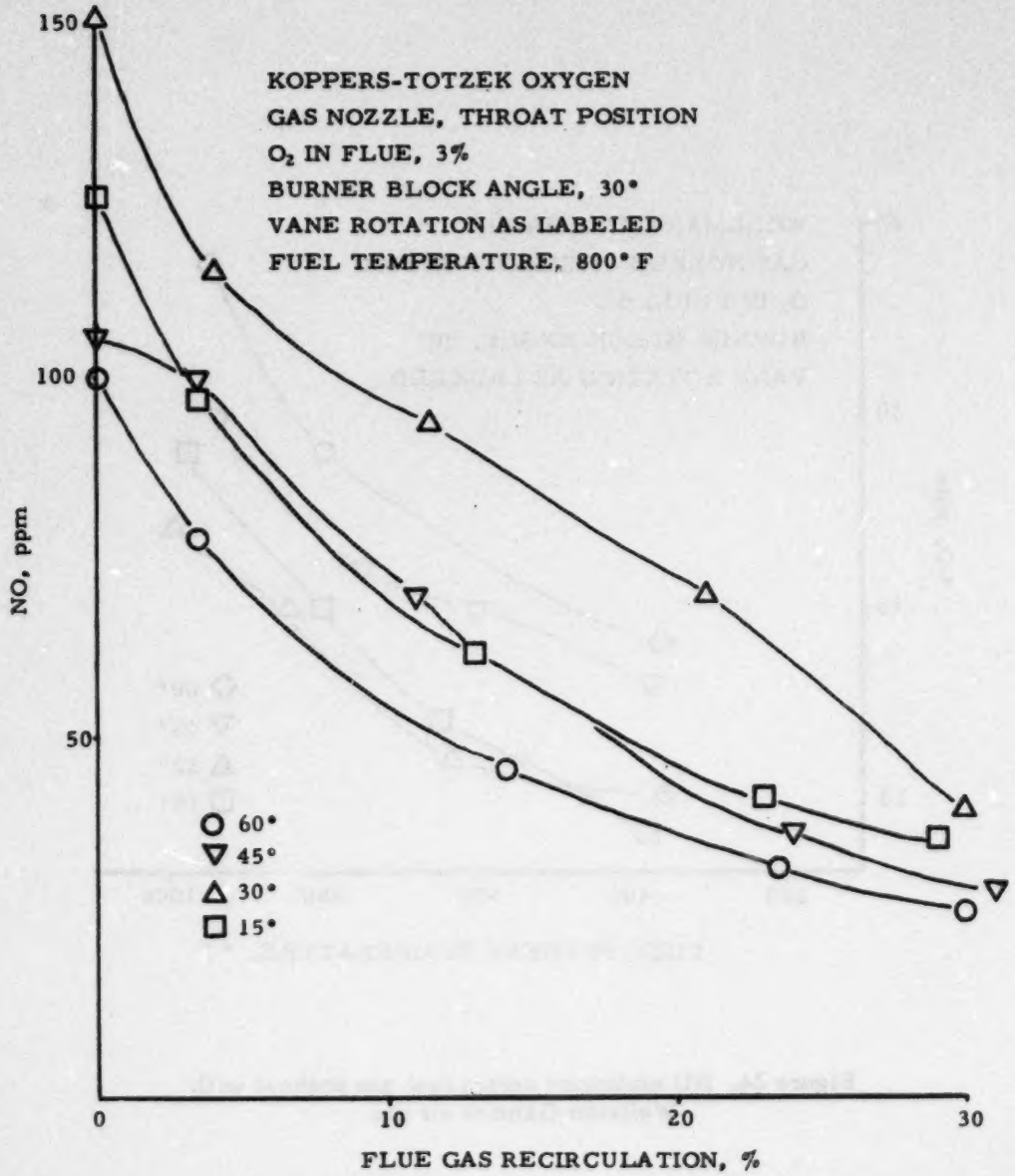

Figure 23. NO emissions versus FGR for Koppers-Totzek oxygen fuel preheated to 800°F

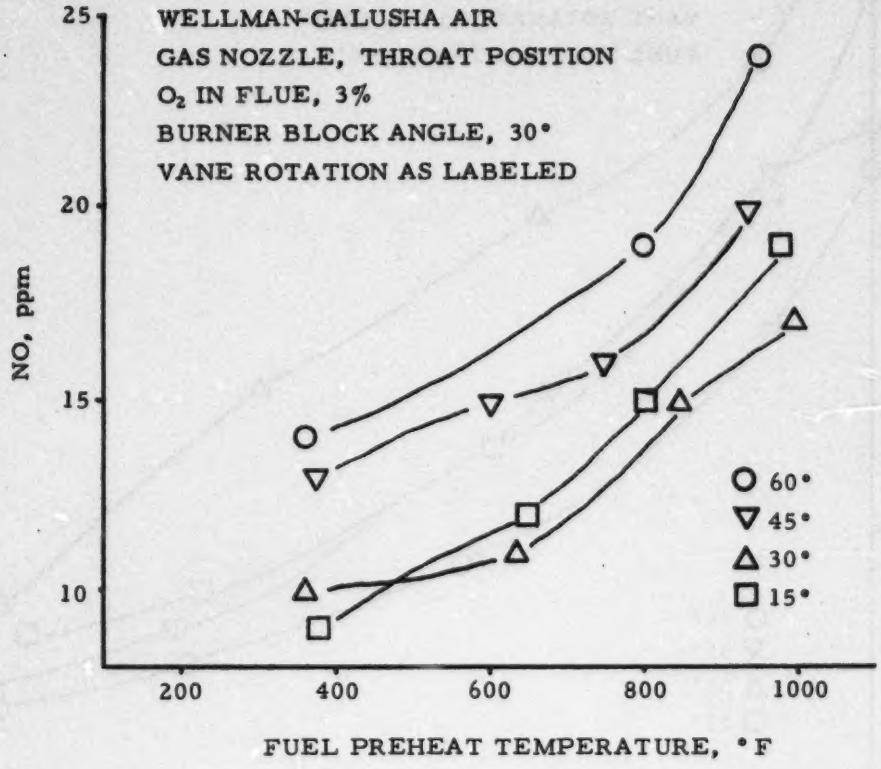

Figure 24. NO emissions versus fuel gas preheat with Wellman-Galusha air gas

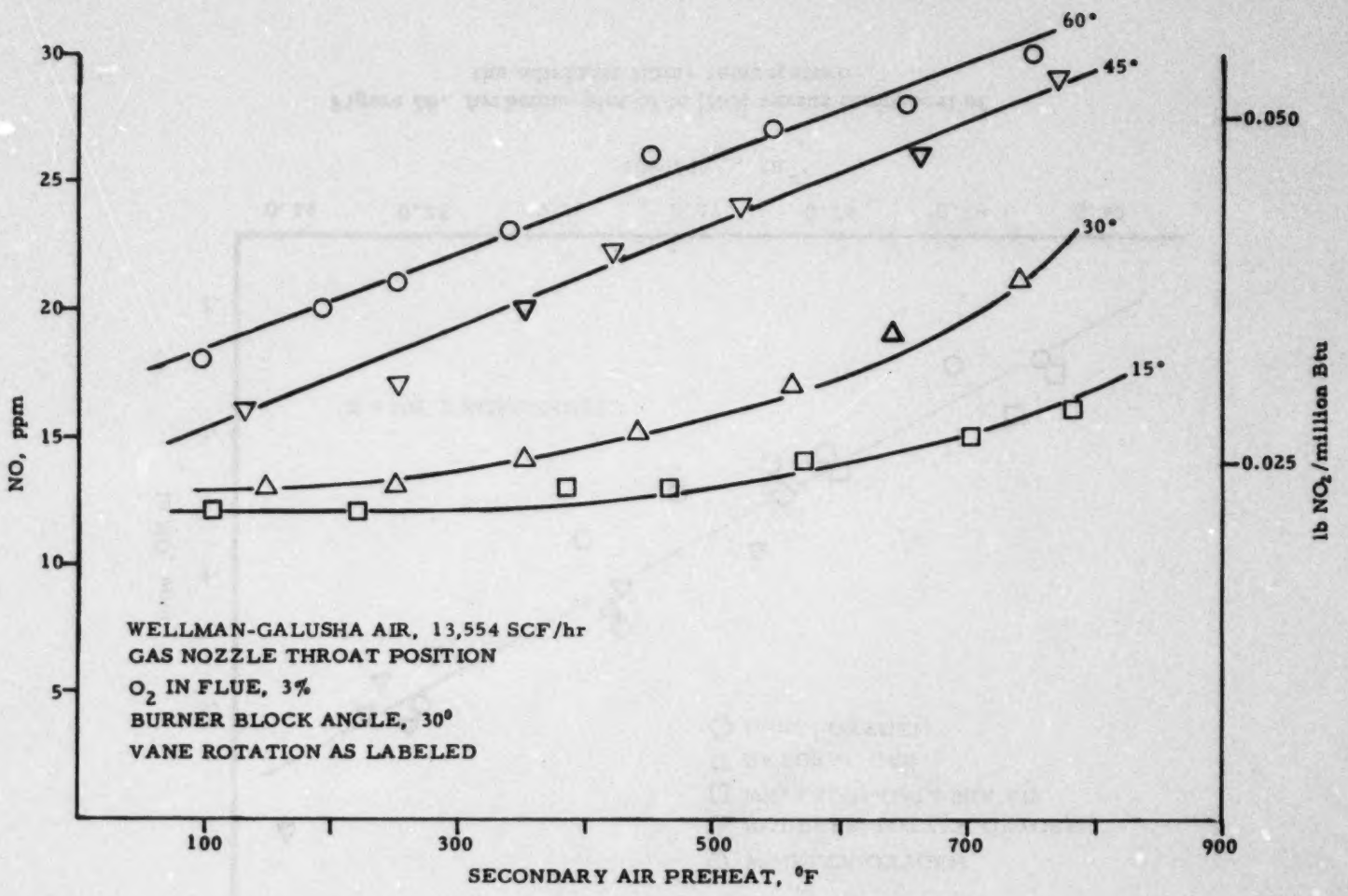

Figure 25. NO emissions versus secondary air preheat with Wellman-Galusha air gas

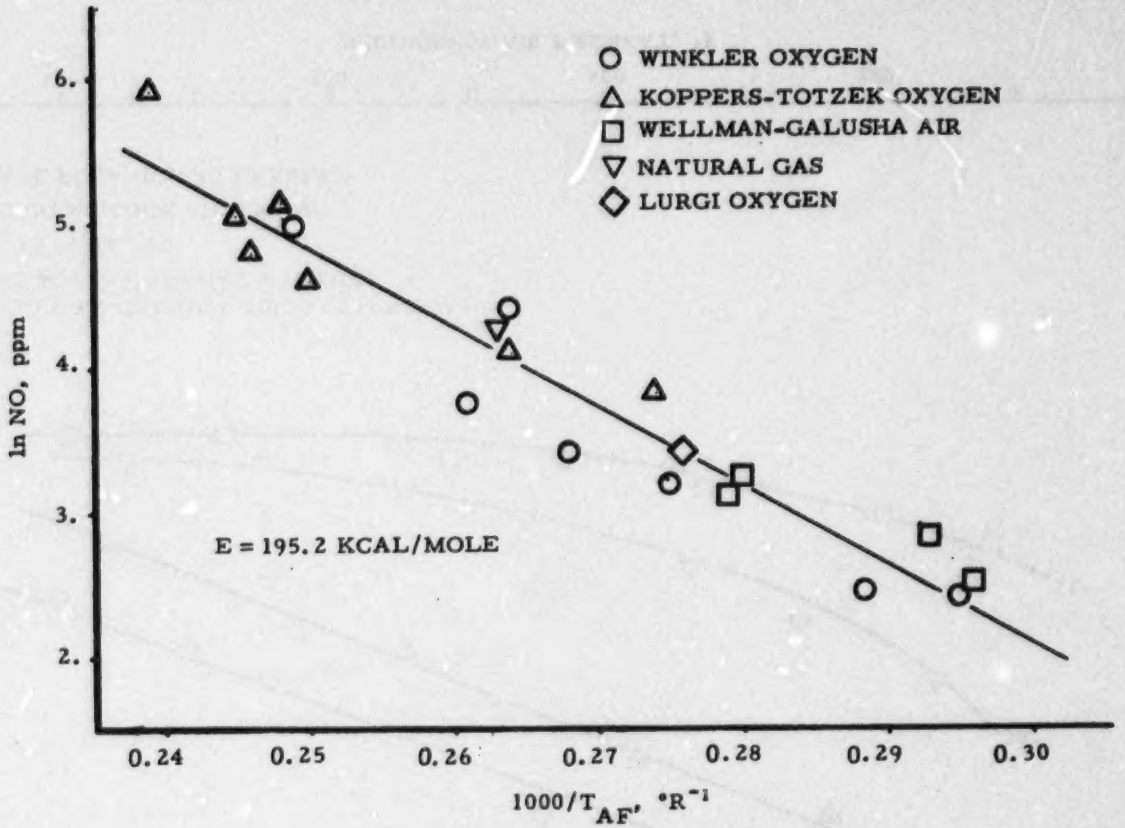

Figure 26. Arrhenius plot of ln [NO] versus reciprocal of the adiabatic flame temperature

FGR and also data from the ambient fuel tests reported earlier. The good correlation obtained suggests that the reaction can be described by an Arrhenius rate expression that uses the adiabatic flame temperature:

$$\ln [NO] \propto -E_A/RT_{AF} \quad (1)$$

Further, if we accept that the true activation energy is 134.7 kcal/mole, as recommended by Thompson, Brown, and Beer[1], we can state the following –

$$\frac{-134.7}{RT_{RXN}} = \frac{-134.7}{RCT_{AF}} \quad (2)$$

so that the rate-controlling reaction temperature is a constant factor of the adiabatic flame temperature. Then, from our plot –

$$\frac{-134.7}{RC} = \frac{-195.2}{R} \quad (3)$$

and thus –

$$C = 0.690 \quad (4)$$

Our plot, therefore, would suggest that the rate-controlling reaction temperatures, T_{RXN}, equal 0.69 T_{AF}. Such temperatures are low compared to those seen in the furnace. This plot, however, appears to be a good empirical method of predicting NO emissions as a function of operating variables, including fuel and air preheat and FGR.

TEMPERATURE PROFILES

To determine the difference in flame temperature reached within the furnace, temperature profiles were taken as a function of fuel type and fuel input conditions. These data were collected for operating conditions yielding the highest measured level of NO emissions. The fuels tested included natural gas (baseline conditions), Koppers-Totzek oxygen, Koppers-Totzek oxygen preheated to 800°F, and Koppers-Totzek oxygen preheated to 800°F with 15% flue-gas recirculation.

All gas temperature mesurements reported were gathered using a suction pyrometer. The head of the pyrometer consisted of a thermocouple (Pt-Pt Rh

---

1 Thompson, D., Brown, T. D. and Beer, J. M., "NO_x Formation in Combustion," Combust. Flame 20, 69-79 (1972) September.

10%) protected by refractory radiation shields. These shields are fitted to the end of a water-cooled probe through which gases are sucked and the thermocouple wires passed. The efficiency of the pyrometer was determined to be 99% using the technique presented by T. Land (Instruments and Automation. Vol. 29, No. 7, 1956).

Baseline data were collected for natural gas at seven axial positions for a 45-degree burner vane rotation. These data are plotted in Figure 27. The axis of the flame was located at the 15.2-cm axial position by making several radial scans at different vertical positions. The flame center line was then confirmed by gas analysis.

Koppers-Totzek oxygen (KTO) has a 241°F higher adiabatic flame (3578°F) temperature than natural gas (3337°F). The KTO yielded a 110°F higher maximum average temperature than natural gas. This difference has been reduced to 70°F in the flue due to wall-gas temperature equilibrium. These temperature profiles are shown in Figure 28.

Koppers-Totzek oxygen gas preheated to 800°F (3605°F adiabatic flame temperature) temperature data are presented in Figure 29. The maximum average temperature is 250°F higher than natural gas. The flue-gas temperature is 240°F higher, while the wall temperature is 198°F higher than those temperatures measured during the combustion of natural gas.

Adding 15% FGR to the Koppers-Totzek oxygen gas preheated to 800°F (KTO 800°F) produced the temperature profile data illustrated in Figure 30. The adiabatic flame temperature (3335°F) is comparable to that of natural gas (3337°F). The maximum average temperature was 37°F higher than for natural gas, while the flue-gas temperatures were similar.

FLAME EMISSIVITY DETERMINATION

Using the pyroelectric radiometer with a 16-inch-diameter cooling target, data were collected for evaluating gas absorptivity. The Schmidt method was employed to reduce the measured data into absorptivities. The following measurements were made for each data point:

R_1 = radiation intensity of flame backed by a cold black target
$= e_f E_f$

R_2 = radiation intensity of a hot black target
$= E_r$

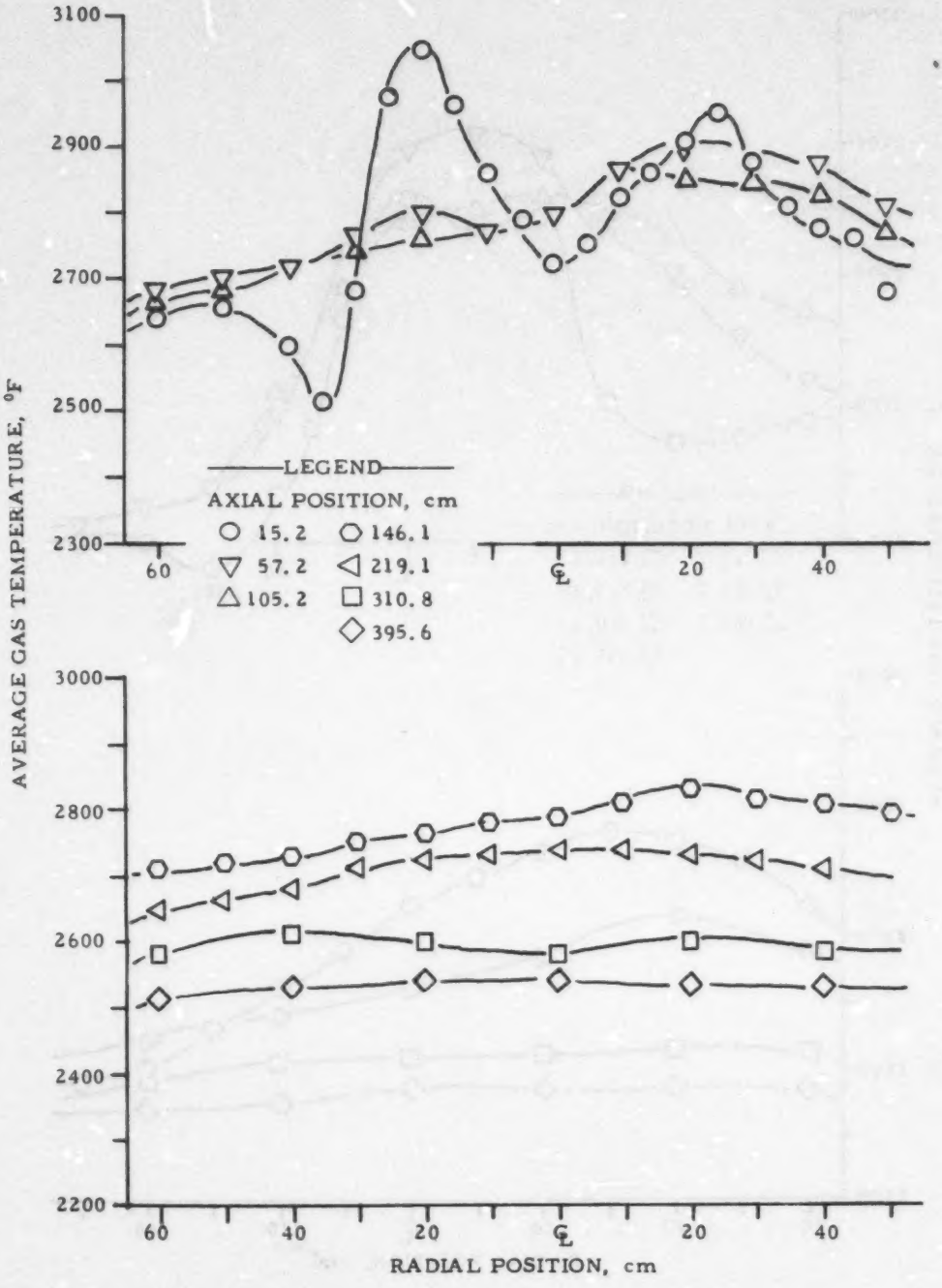

Figure 27. Average gas temperature profile for natural gas with a 45-degree vane rotation

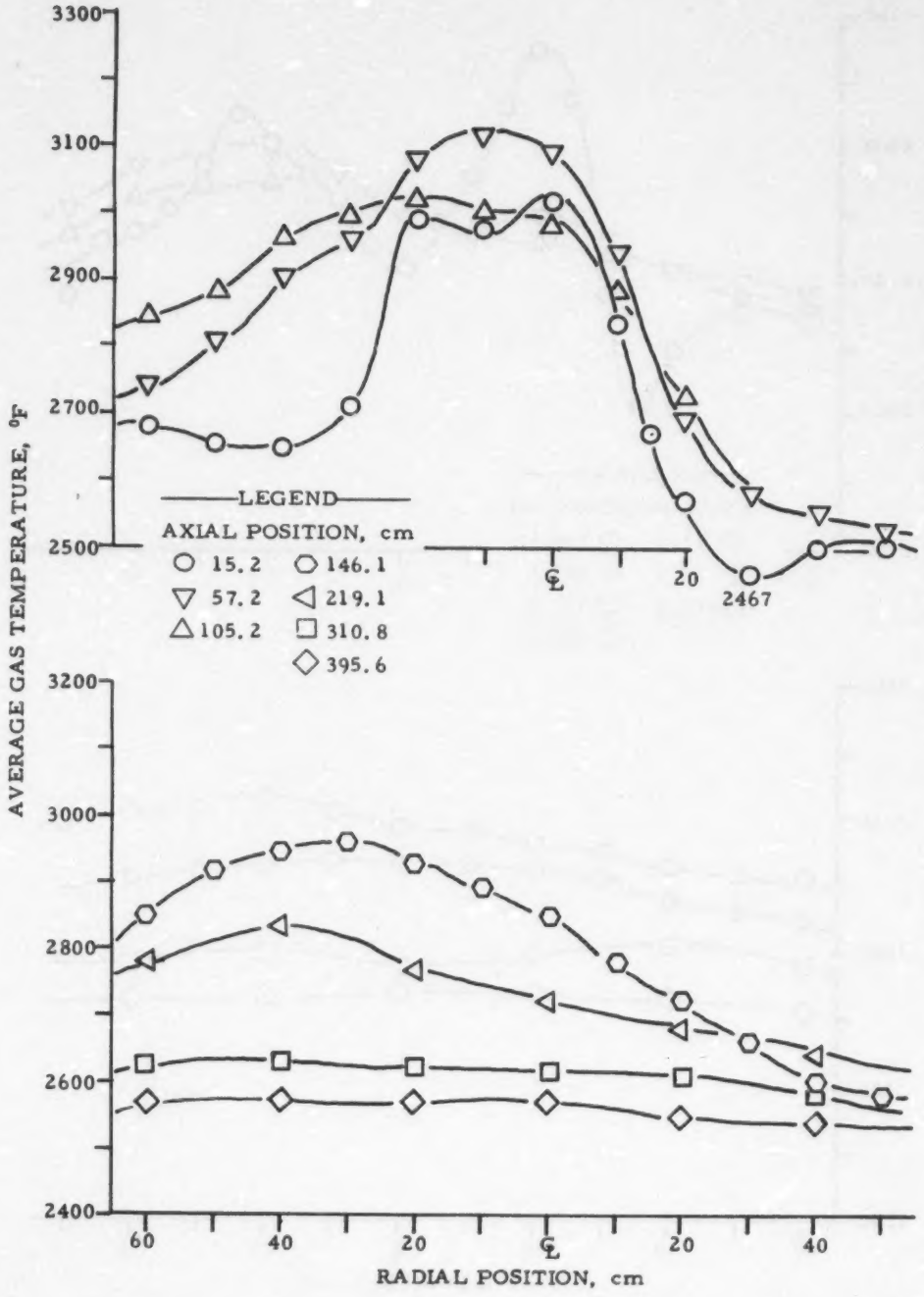

Figure 28. Average gas temperature profile for "ambient" Koppers-Totzek oxygen gas with a 45-degree vane rotation

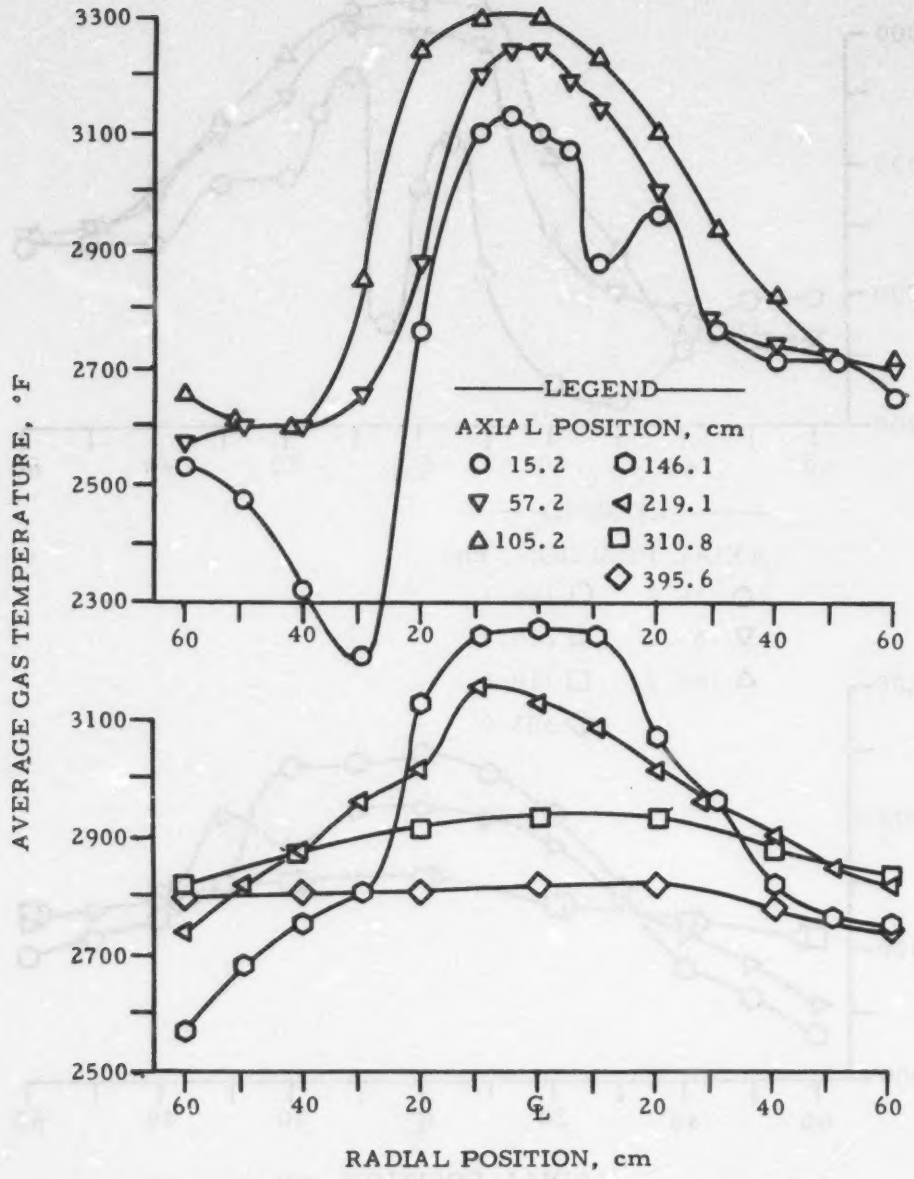

Figure 29. Average gas temperature profile for preheated Koppers-Totzek oxygen gas with a 45-degree vane rotation

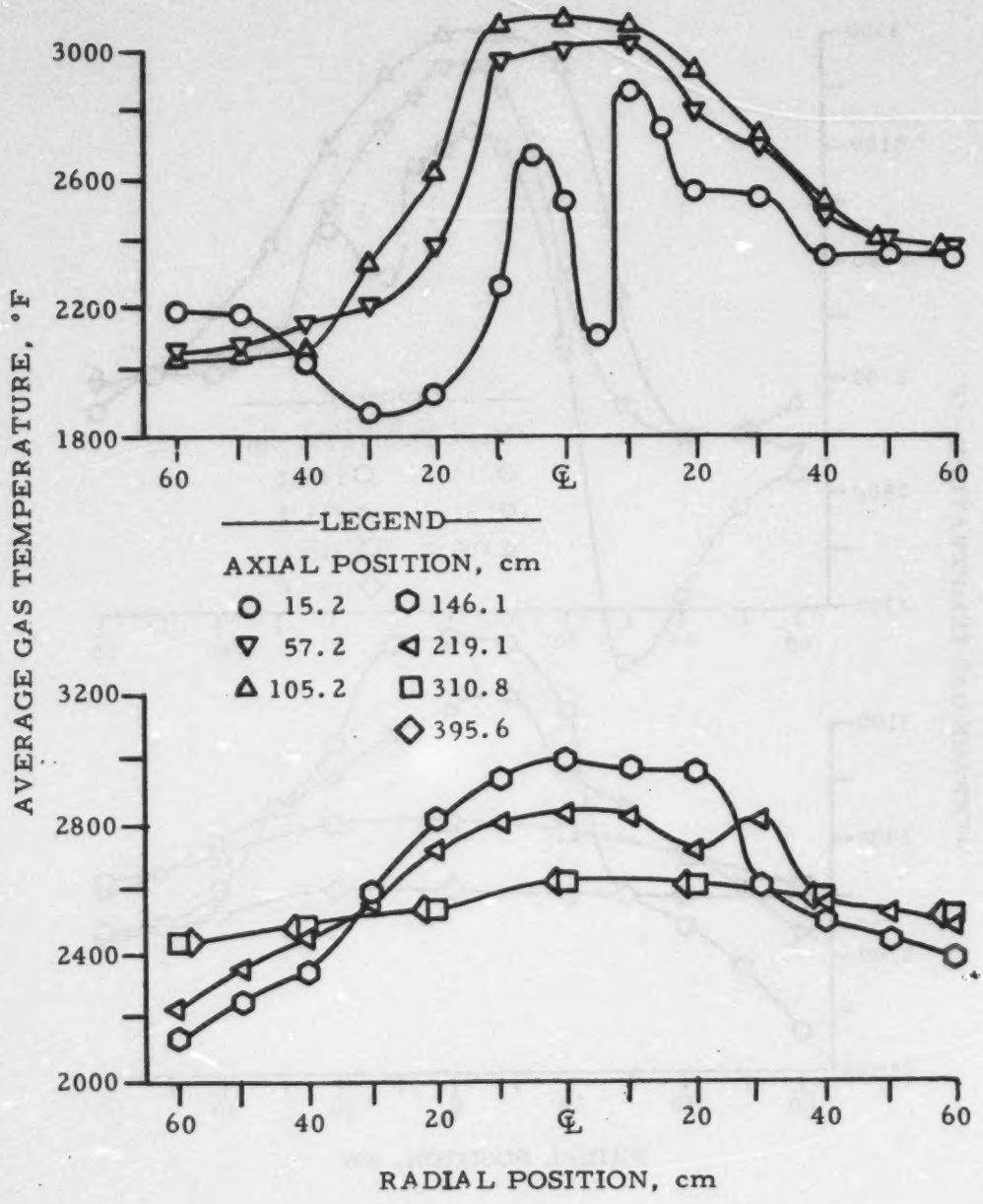

Figure 30. Average gas temperature profile for preheated Koppers-Totzek oxygen gas with 15% FGR with a 45-degree vane rotation

R_3 = radiation intensity of a flame backed by a hot black target
$= e_f E_f + (1 - a_f) E_r$

where e_f is the flame emissivity, a_f is the flame absorptivity for radiation originating at the hot target, and E_f and E_r are the black body emissive powers (σT^4) at the flame and hot target temperatures. It follows that –

$$a_f = 1 - \frac{R_3 - R_1}{R_2}$$

As the target temperature T_r is usually colder than the flame temperature T_f, and given the properties of nonluminous flame radiation, it is expected that $a_f > e_f$. The relationship between a_f and e_f can be found in Hottel and Sarofim[2] as –

$$\frac{a_f}{e_f} = \left(\frac{T_r}{T_f}\right)^{a+b-c}$$

Values of a+b–c can be estimated from Hottel and Sarofim's plots of CO_2 and H_2O.

R_2 is measured from a hot refractory surface that is not black; thus the measured radiation intensity contains reflected as well as emitted radiation. When siting on a refractory of reflectivity ρ_r, one measures a leaving flux density W_r (the apparent emissive power) equal to the sum of the emitted radiation $e_r E_r$, and the reflected radiation $p_r H_r$ is the flux density incident on the refractory in question. When there is no flame, the value of H_r is simply the flux density W_r leaving the refractory surfaces viewed from the reference spot. When there is a flame, the value of H_r is equal to the sum of the flame radiation $\varepsilon_f E_f$ and the radiation received from other refractory surfaces after attenuation by the flame $(1 - \varepsilon_f)W_r$. The three measurements for the Schmidt are then –

1. Flame with cold black background: $R_1 = \varepsilon_f E_f$

2. Hot refractory: $R_2 = W_r = \varepsilon_r E_r + \rho_r H_r = \varepsilon_r E_r + \rho_r W_r = E_R$

3. Flame backed by hot refractory: $R_3 = \varepsilon_f E_f + (1 - \varepsilon_f) W^*_r$

---

[2] Hottel, H. C. and Sarofim, A. F., Radiative Transfer, 300, New York: McGraw-Hill, 1967.

$$= \varepsilon_f E_f + (1 - \varepsilon_f) \left[\varepsilon_r E_r + \rho_r H_r \right)$$

$$= \varepsilon_f E_f + (1 - \varepsilon_f) \left\{ \varepsilon_r E_r + \rho_r \left[\varepsilon_f E_f + (1 - \varepsilon_f) W^*_r \right] \right.$$

$$= \varepsilon_f E_f + (1 - \varepsilon_f) \left\{ \varepsilon_f E_r + \rho_r \left[\varepsilon_f E_f + (1 - \varepsilon_f) \left(\frac{\varepsilon_r E_r + \rho_r \varepsilon_f E_f}{1 - \varepsilon_r (1 - \varepsilon_r)} \right) \right] \right.$$

Applying the Schmidt method as before:

$$a_f = 1 - \frac{R_3 - R_1}{R_2}$$

the following expression for absorptivity is derived:

$$\alpha_f = 1 - (1 - \varepsilon_f) \left\{ \varepsilon_r + \rho_r \left[\varepsilon_f \frac{E_f}{E_r} + (1 - \varepsilon_f) \left(\frac{(\varepsilon_r + \rho_r \varepsilon_f \frac{E_f}{E_r})}{1 - \rho_r (1 - \varepsilon_f)} \right) \right] \right\} \tag{5}$$

To quantify the refractory reflectivity, the radiometer was sited on a hot refractory furnace sidewall through the general probe holder (Figure 11) and then with the probe holder removed. All precautions were taken to ensure that the radiometer view angle was identical both with and without the probe holder and that the cold probe holder did not change the refractory temperature during the measurements. Figure 31 presents data collected during these reflectance trials plotted against the refractory emissivity data proved by Babcock and Wilcox (solid line).

To evaluate the gas composition emissivity using Equation 5, the following experimental data must be collected: 1) R_1, R_2, and R_3 are measured using the pyroelectric radiometer and water-cooled black target; 2) a_f is then calculated using the Schmidt technique; and 3) the furnace wall temperature is measured using an optical pyrometer. These measured data are used in conjuction with Figure 31 to evaluate ε_r and ρ_r (refractory emissivity and reflectivity). The final item of information needed to use Equation 5 is the flame temperature (T_f).

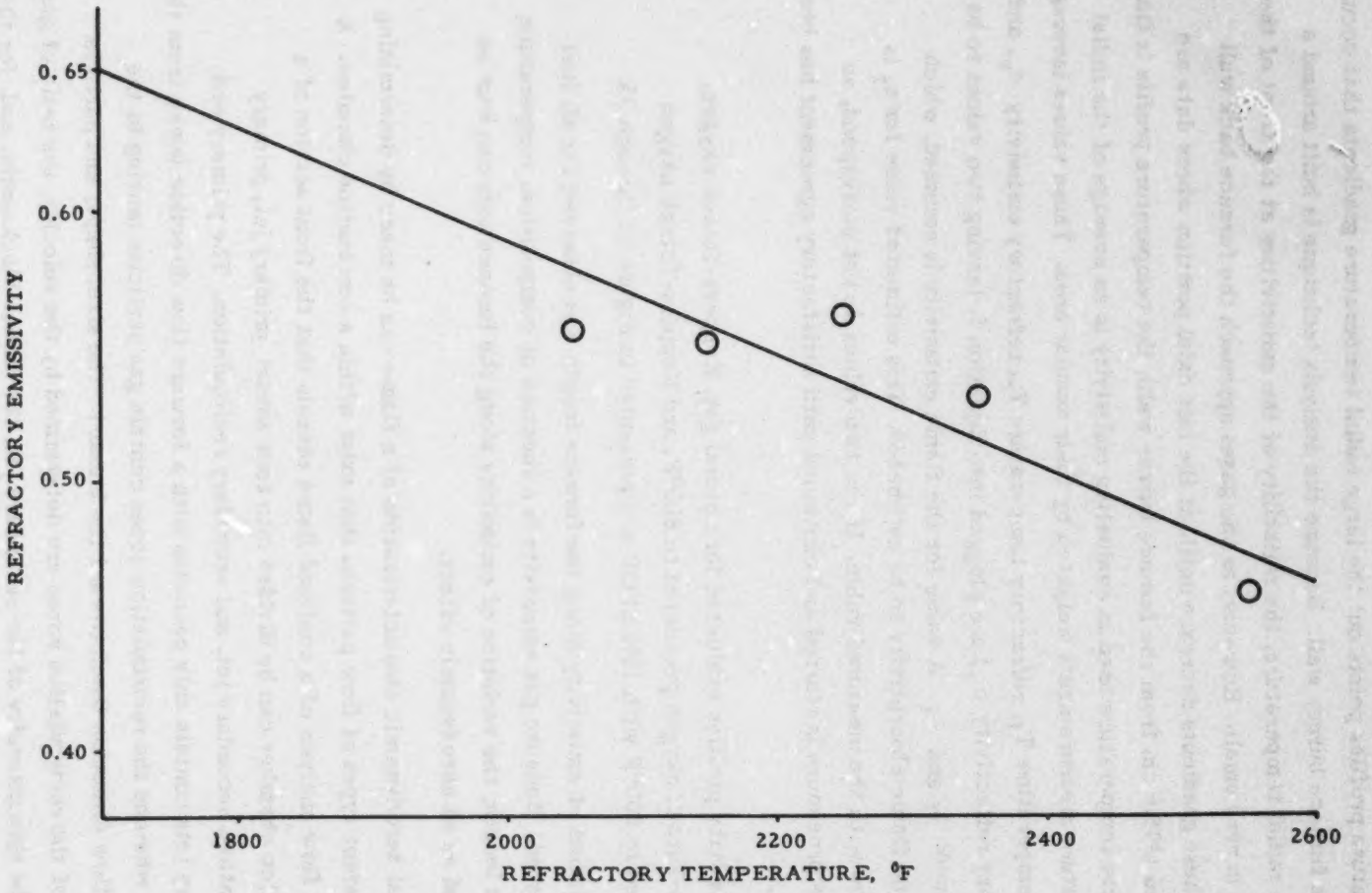

Figure 31. Refractory emissivity versus refractory temperature

These data were presented in Figures 27 through 30. A review of these temperature profiles points out the large radial temperature gradients that occur near the furnace burner wall. Because the analysis technique is built around a uniform radial temperature, the reliability of the emissivities at the front of the furnace is very small. However, as the gases approach the furnace back wall (flue), these gradients decrease until, at the last axial position where data are collected (395.6 cm from the furnace burner wall), the temperature profile is flat. The flame temperature used in evaluating emissivity is an average of the radial temperature measurements weighted by their annular area. These values (average flame temperature T_f, refractory temperature T_r, refractory emissivity ε_r, and refractory reflectivity ρ_r) are plugged into Equation 5, leaving two values to be determined: a_f and ε_f. A value for the flame emissivity is assumed, which allows the flame absorptivity to be estimated. This estimated value for a_f is compared with the measured value. If the two values do not correspond, an iterative procedure is started and continued until satisfactory agreement has been reached.

The emissivity profiles evaluated for natural gas, Koppers-Totzek oxygen, Koppers-Totzek oxygen preheated to 800°F, and Koppers-Totzek oxygen preheated to 800°F with 15% EFGR are presented in Figure 32 through 35.

The variation of emissivity along the furnace length was observed for all fuel gases tested. Because gas emissivity is a function of composition, temperature, and path length, the variation of emissivity along the furnace axis can best be explained as an aerodynamic effect.

A general aerodynamic characterization of a flame can be made by determining the different types of flow patterns that exist within a combustion chamber. A detailed flow analysis of a confined flame reveals that the front section of a combustion chamber can be divided into four zones: primary jet, primary recirculation, secondary jet, and secondary recirculation. The primary and secondary jets contain only particles with a forward flow direction (away from the burner), whereas the recirculation zones contain gas particles moving in the reverse flow direction (back toward the burner). The size, shape, and particle density of the recirculation zones are determined by the velocity, the ratio of gas to air, the spin intensity of the secondary jet, the burner-block angle, and, for the

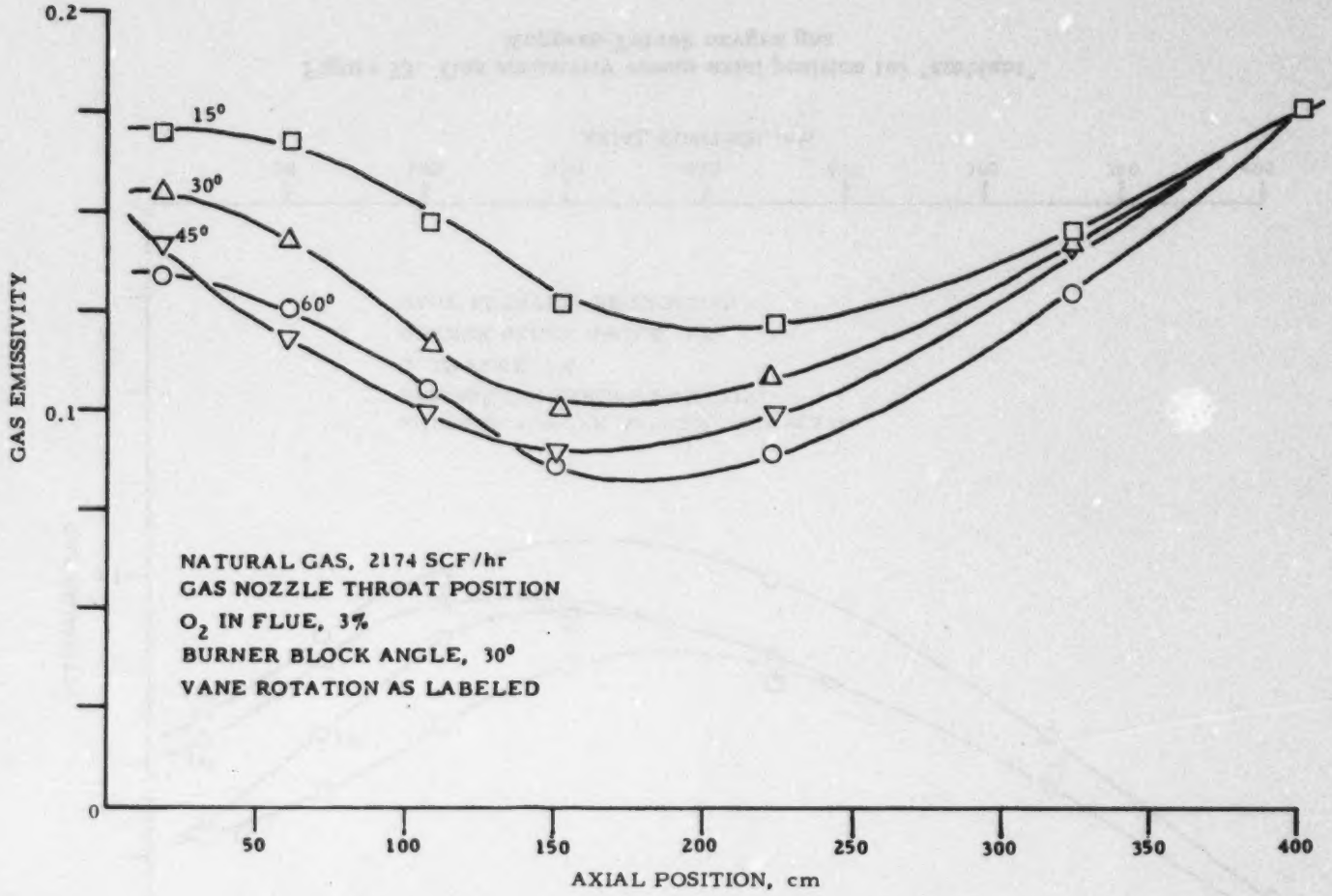

Figure 32. Gas emissivity versus axial position for natural gas

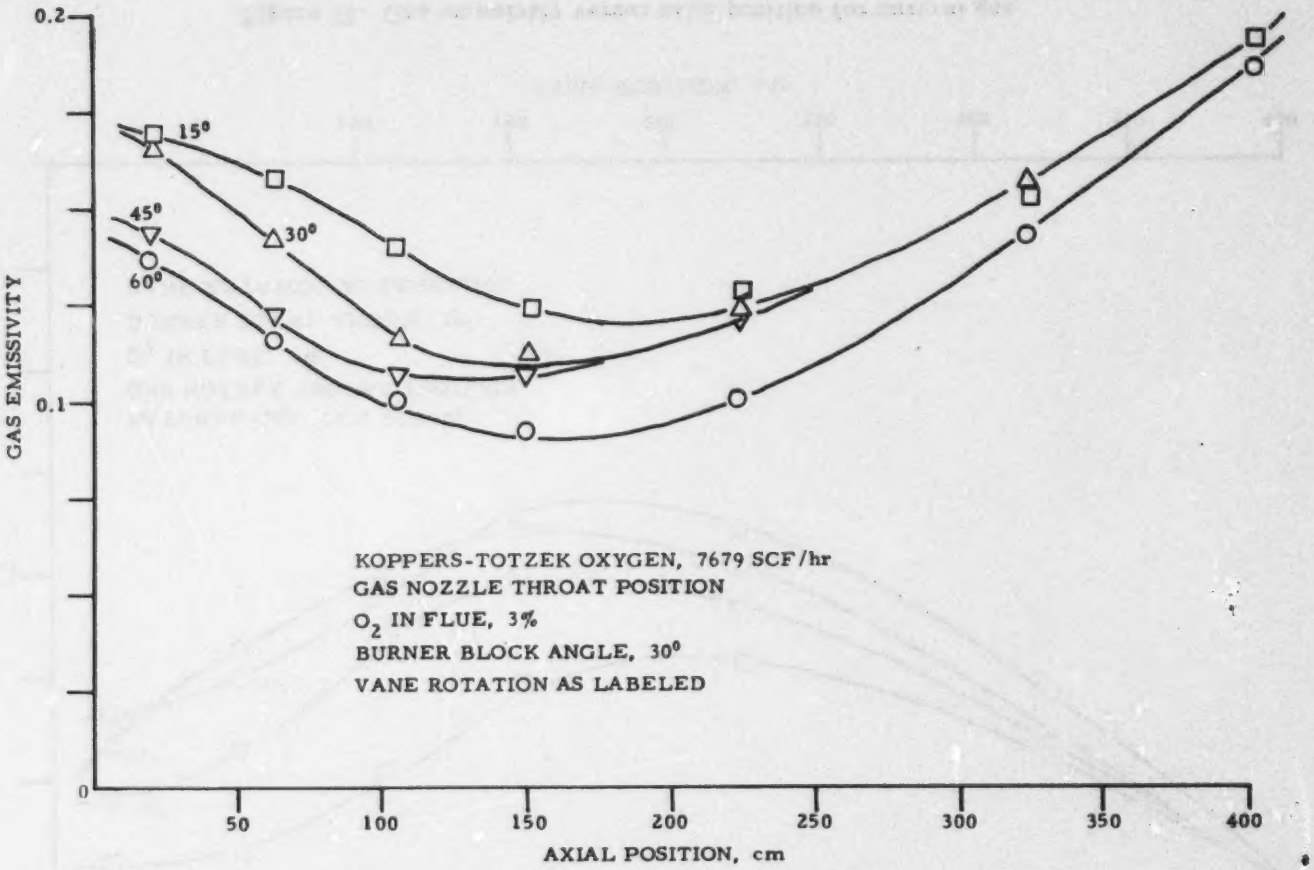

Figure 33. Gas emissivity versus axial position for "ambient" Koppers-Totzek oxygen gas

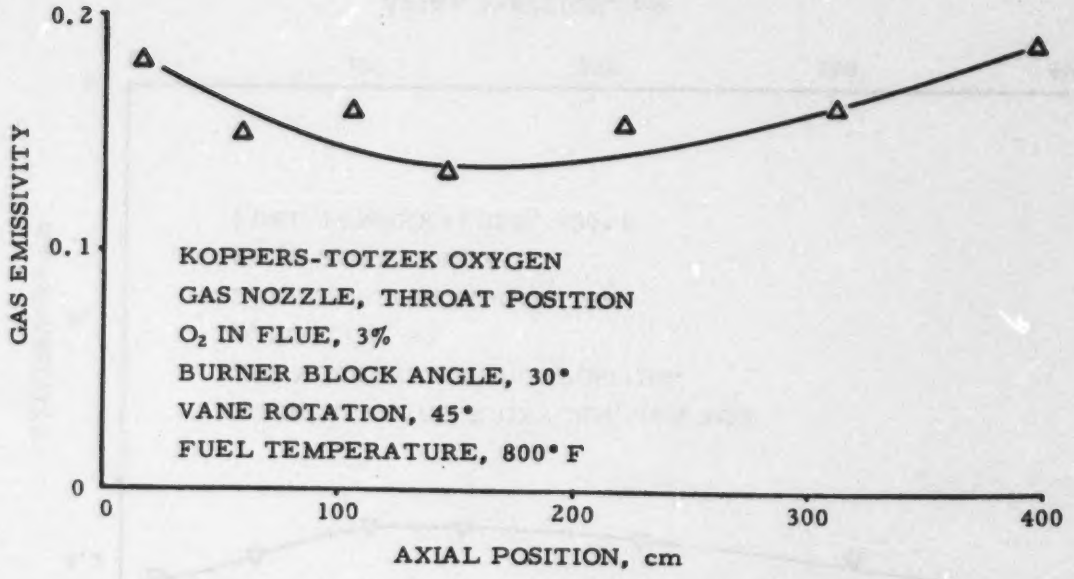

Figure 34. Gas emissivity versus axial position for preheated Koppers-Totzek oxygen gas

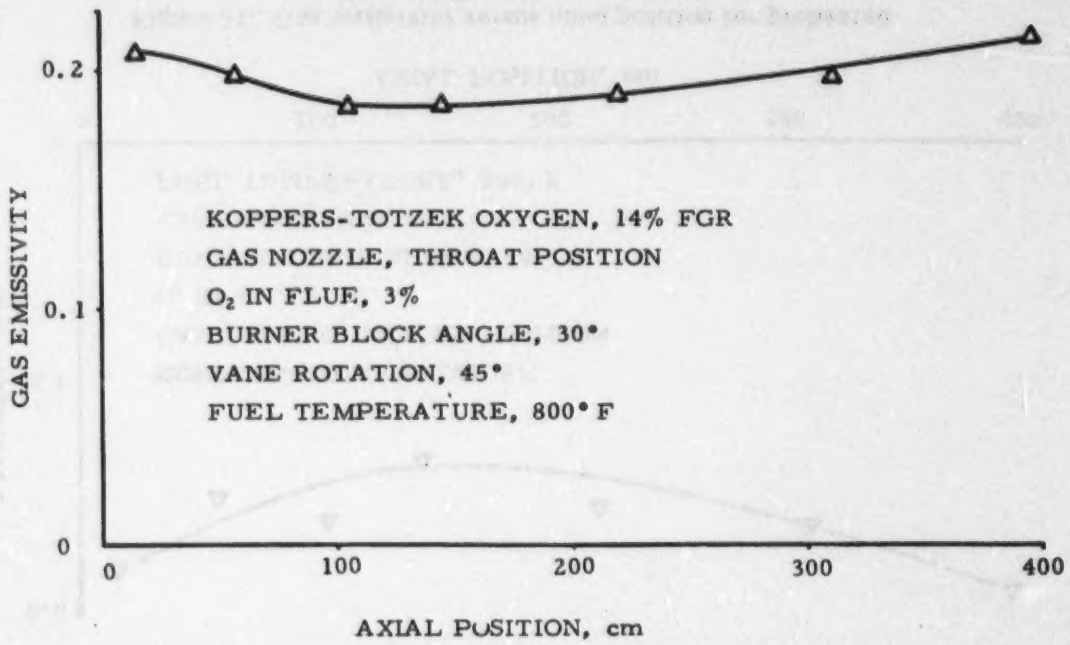

Figure 35. Gas emissivity versus axial position for preheated Koppers-Totzek oxygen gas with 15% FGR

secondary recirculation zone, the size and shape of the combustion chamber. Figure 36 shows the type of flow pattern that was observed during this investigation. This flow pattern is conventionally labeled Type II.

A Type II flow pattern is generated when the secondary jet has a tangential velocity component large enough to cause the particles to adhere to and pack tightly against the burner block. This packing creates a low or negative pressure region in the center of the burner block. The pressure differential between the furnace and the central region of the burner block causes gas molecules to be pulled into this region and back toward the burner, thus creating the primary recirculation zone. When the velocity of the primary jet is greater than the velocity of the recirculating gases in the primary recirculation zone, the primary jet penetrates this reverse flow region, and a recirculation lobe occurs on each side of the burner axis.

A gas analysis of the secondary recirculation zone reveals species concentrations similar to those measured at the furnace flue. Thus, an emissivity measured at the furnace front wall would be an addition of the flame plus secondary recirculation zones. The emissivity from the recirculation zone is approximately that measured at the rear of the furnace. As the flame spreads, the optical path of the secondary recirculation zone is decreased, reducing the concentration of radiating sources. As the combustion continues, the concentrations of CO_2 and H_2O along the optical path are increased as products of combustion. At the end of the furnace, the gas temperatures and species concentrations across the width of the furnace are nearly uniform, and the emissivity is as if from a static mixture at a uniform temperature and composition. This is confirmed by the emissivities measured for natural gas combustion (Figure 32), where the measured emissivity at the front of the furnace is different for each vane angle tested; toward the end of the combustion chamber, however, all the values converged to approximately 0.177.

The variation of emissivity near the furnace front wall as a function of vane angle occurs due to the tangential velocity component of the secondary air – that is, how fast the vortex of combustion air will spread upon leaving the burner block. The larger the tangential velocity component, the higher the rate of post burner-block expansion and the smaller the contribution of the secondary recirculation zone to the measured emissivity.

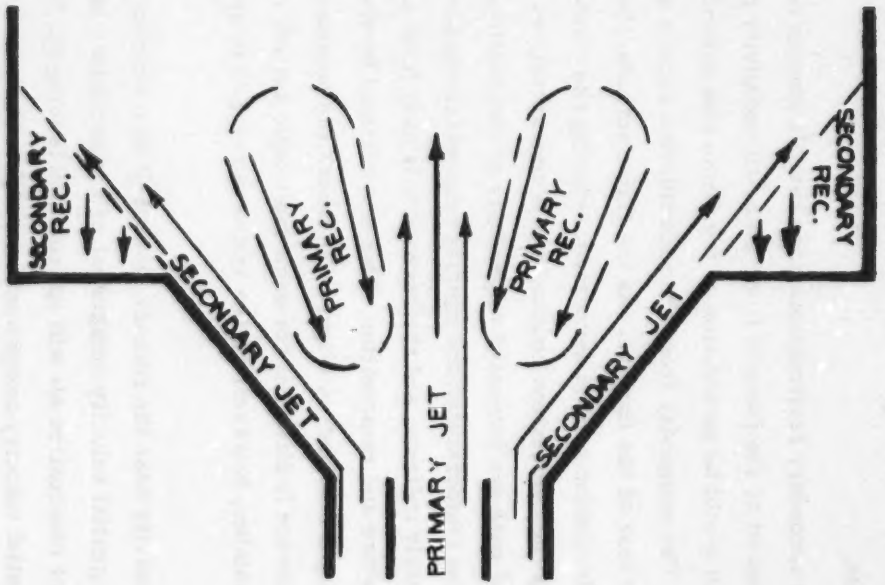

TYPE II

LOW SWIRL INTENSITY
PRIMARY JET VELOCITY
SECONDARY JET VELOCITY

Figure 36. Flame flow pattern tested

Another possibility is that a_f (which is the value measured) increases for some distance into the furnace as a consequence of the presence of either soot or cold pockets of absorbing gas.

Emissivities were calculated using the measured flue-gas temperatures and compositions for a 45-degree vane angle rotation and CO_2 and H_2O vapor emissivities found in Radiative Transfer (Hottel and Sarofim).[2] These calculated values are listed in Table 4. They spread from a minimum of 0.159 for natural gas to a maximum of 0.190 for preheated Koppers-Totzek with 15% FGR. These calculated values are independent of burner operating conditions and the furnace geometry is considered only when evaluating the mean beam length. Since the radiometer viewed a collimated beam, the furnace width corresponds to the beam length.

A second calculation technique developed by Leckner[3] using NASA data was also employed. This method is based on a statistical model using spectral data to evaluate total emissivities of carbon dioxide and water vapor in homogenous gases. For carbon dioxide emissivity there is good agreement with Hottel's emissivities; however, for water vapor, Leckner's emissivities at temperatures above 1650°F are consistently higher and show that the partial pressure connection factor is temperature-dependent. This effect is shown in Table 4 with Leckner's emissivities larger than Hottel's for all the fuel gases tested. The experimentally evaluated emissivities were between the theoretically determined emissivities.

These experimental data do provide a basis for recommending the use of calculated emissivities for extrapolating to the dimensions of commercial boilers.

---

[2] Hottel, H. C. and Sarofim, A. G., Radiative Transfer, 224-37 ,New York: McGraw-Hill, 1967.

[3] Leckner, B., Combustion and Flame 19:33, 1972.

Table 4. CALCULATED AND MEASURED EMISSIVITIES

ϵ_{calc} = calculated emissivity
a'_{meas} = measured absorptivity
ϵ_{meas} = measured emissivity
Difference = $\frac{|\epsilon_{calc} - \epsilon_{meas}|}{\epsilon_{calc}}$

Fuel	P_{CO_2}	P_{H_2O}	Gas temp, °R	a'_{meas}	ϵ_{meas}	Hottel-Sarofim		Leckner	
						Emissivity	%Δε	Emissivity	%Δε
Natural gas	0.083	0.167	3013	0.131	0.177	0.159	+11	0.215	−18
Koppers-Totzek oxygen	0.204	0.121	3014	0.145	0.190	0.174	+9	0.211	−10
Koppers-Totzek oxygen, 800°F	0.198	0.143	3256	0.129	0.192	0.161	+19	0.202	−5
Koppers-Totzek oxygen, 800°F plus 15% FGR	0.198	0.143	2996	0.164	0.215	0.190	+13	0.215	0

DATA CORRELATION

NO EMISSIONS

Due to the size of the gas-generating system for synthesizing the medium- and low-Btu test gases, the firing density of the pilot-scale test furnace could not exceed 6923 Btu/ft^3-hr. To permit a better correlation as to the level of emissions that could be anticipated from a utility boiler, natural gas was fired with inputs up to 3.75 million Btu/hr. This corresponds to a firing density of 11,538 Btu/ft^3-hr, which produced a NO emission level of 225 ppm compared with the New Source Perfomance Standard for natural gas at 1000 Btu/SCF of 168 ppm (0.2 pounds NO_2/million Btu heat input). These data are graphed in Figure 37.

A 300-MW utility boiler with a radiant chamber 30 x 60 feet in cross section and 80 feet high is fired with 2.86 X 10^9 Btu/hr. The firing density for a boiler of this size at this firing rate is 19,860 Btu/ft^3-hr. Extrapolating the data of Figure 37 yields a NO emission level for the 19,860 Btu/ft^3-hr firing density of 458 ppm. To quantify the anticipated NO emission levels from this 300-MW boiler for each of the fuel gases tested, it is assumed that an identical firing density-to-NO emission level relationship would occur for each medium- and low-Btu gas as is represented for natural gas in Figure 37. From this assumption, the NO emission levels presented in Table 5 were projected.

Thus, only two fuel gases tested were projected to comply with the 0.2 lb NO_2 per million Btu performance standard with the burner system operating normally. High temperature (800°F) Winkler oxygen combustion with 15% FGR in the combustion air will meet the existing standard. The compliance results from a 2933°F adiabatic flame temperature which is 335°F lower than high temperature Winkler oxygen gas with no FGR, and 394°F lower than ambient Winkler oxygen gas. Thus it appears that all gases with an adiabatic flame temperature above 3250°F will require modifications to the burner/boiler system in order to comply with the source performance standards.

FURNACE PERFORMANCE

The efficiencies evaluated on the pilot-scale furnace for each of the fuels tested are listed in Table 6. These efficiencies (defined as the fraction of total input

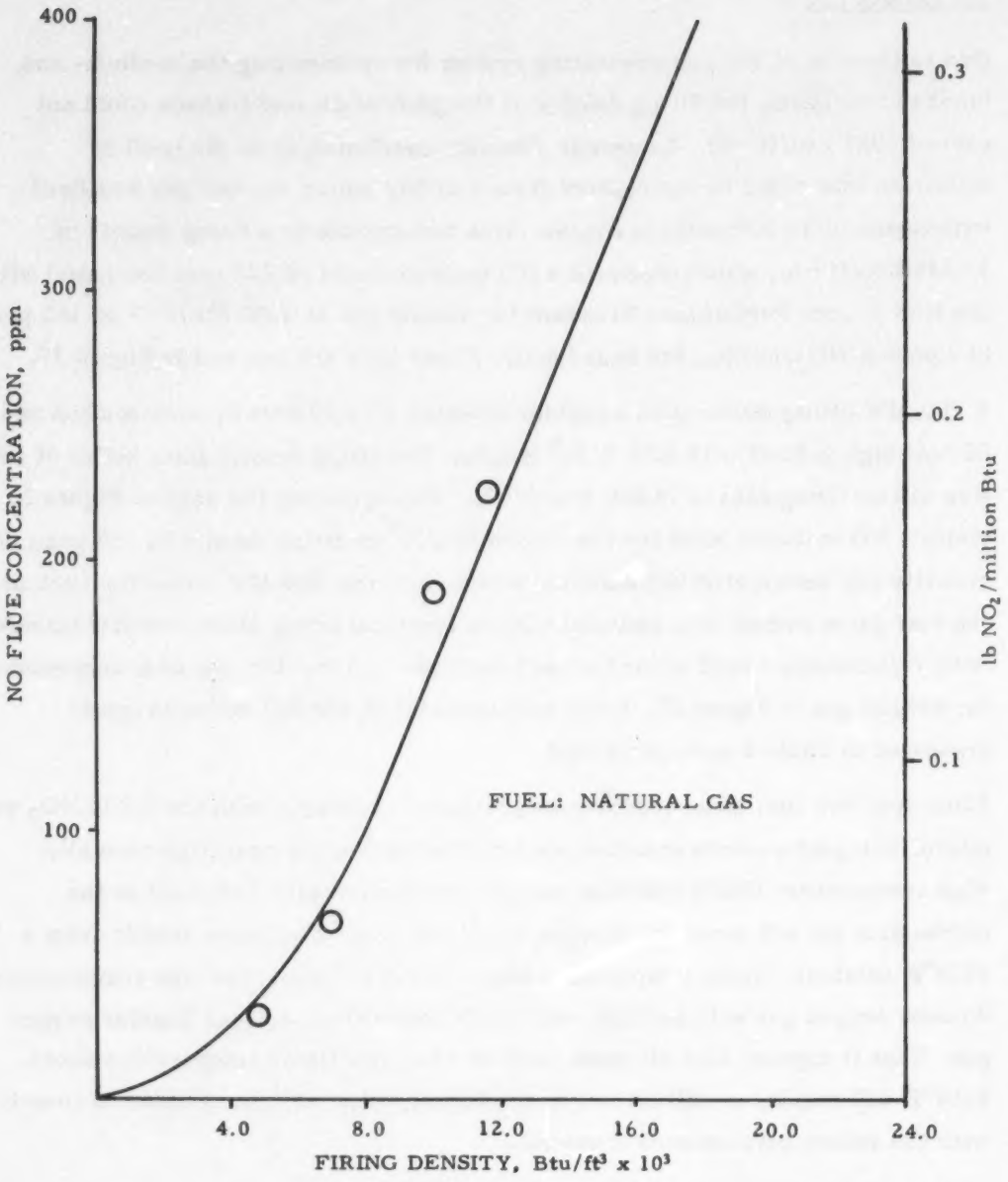

Figure 37. NO emissions versus firing density for the pilot-scale furnace

Table 5. PROJECTED NO EMISSION LEVELS FOR A UTILITY BOILER

Fuel	NO, ppm	lb $NO_2/10^6$ Btu	Adiabatic flame temp, °F
Natural gas	458	0.714	3337
Winkler oxygen	514	0.766	3327
Winkler oxygen, 800 °F preheat	183	0.289	3268
Winkler oxygen, 800 °F preheat plus 15% FGR	70	0.129	2933
Koppers-Totzek oxygen	733	1.019	3578
Koppers-Totzek oxygen, 800 °F preheat	972	1.372	3605
Koppers-Totzek oxygen, 800 °F preheat plus 15% FGR	317	0.524	3335
Wellman-Galusha air	106	0.198	2948
Wellman-Galusha air, 800 °F preheat	113	0.208	3026

enthalpy given up in the furnace by the combustion products) can be evaluated using the flue-gas temperatures in in Table 6 and the combustion products in Table 1. Subtracting the flue-gas enthaply from the total enthalpy input gives the amount of heat transferred in the furnace, and dividing by the total enthalpy input gives the efficiency. The pilot-scale furnace efficiencies for natural gas, Koppers-Totzek oxygen, preheated Koppers-Totzek oxygen, and preheated Koppers-Totzek oxygen plus 15% FGR are within the range of 28.2% to 34.2%.

In addition to changes in the furnace (radiant section) efficiency when natural gas is replaced with a low-Btu gas, the temperature and volume of combustion gas products entering the convective section will change, thus varying the amount of heat absorbed in the convective section. Comparing the volume of combustion products for the test fuels reveals that Koppers-Totzek oxygen (293 Btu/ft^3) has a 9% smaller volume of combustion products than natural gas, while Winkler air (116 Btu/ft^3) produces a 42% greater volume of combustion products than natural gas. These changes in combustion-product volume will result in changes in gas velocities and shift the heat absorption patterns within the convective section.

Table 6. PILOT-SCALE FURNACE EFFICIENCIES FOR PREHEATED FUEL GASES

Fuel	Flue-gas temp, °F	Furnace efficiency, %
Natural gas	2553	28.6
Koppers-Totzek oxygen, 800 °F	2592	34.2
Koppers-Totzek oxygen, 800 °F plus 15% FGR	2681	28.2

To evaluate a shift in heat absorption when retrofitting a boiler with low-Btu gas requires a method of calculation. Babcock and Wilcox Co. (B&W) agreed to take experimental data presented in EPA Report No. 600/7-77-094a and use them for the input conditions to the convective section to predict differences in overall boiler efficiency (radiant plus convective) between natural gas and low-Btu gases. The method of calculation employed by B&W was to use their design computer program to forecast changes in boiler performance when retrofit with a low-Btu fuel gas.

The particular boiler selected for their calculations was a standard design with a maximum rated steam flow of 2,430,500 lb/hr at 2620 psig/1005°F at the superheater outlet when fired with natural gas. The unit (B&W Contract RB-455) is installed at the Teche Station of the Central Louisiana Electric Co. and supplies steam to a Westinghouse turbine having a maximum capacity of 361 MW. This same unit was reported on by B&W for EPRI Project 265-2, entitled "Low Btu Gas Study," a program designed to look at retrofitting boilers using only existing design information.

To update these results, the flue-gas temperatures and gas compositions measured on the IGT furnace during earler "ambient" temperature fuel-gas trials were used as input data. These temperatures and gas compositions were assumed to be identical to those entering the convective section of the boiler. Using these experimental results, B&W calculated unit efficiencies for natural gas, Winkler oxygen, and Winkler air fuel gases. The total required output of Unit RB-455 based on a 2,198,000 lb/hr main steam flow is 2652.5 million Btu/hr. Based on the experimental data and fuel analysis presented in Table 1, B&W generated the information in Table 7. The first line shows natural gas firing with the amount of excess air that the unit was designed for at this load. The second line shows natural gas firing with input conditions (325°F air preheat and 3% excess oxygen) identical to those used for the pilot-scale test furnace. The actual output from firing natural gas with the increased level of excess air is in excess of 2652.5 million Btu/hr. This is because higher gas weights result from the increased volume of combusiton air creating an overabsorption in the reheater. Similar reheat overabsorption occurs in the output for Winkler air, which is also greater than 2652.5 million Btu.

Table 7. B&W CALCULATED BOILER EFFICIENCIES USING IGT DATA

Fuel	IGT flue-gas temp, °F	Actual unit output, 10^6 Btu/hr	Unit efficiency, %	O_2 in flue gas, % by vol	B&W furnace exit-gas temp, °F
Natural gas	--	2652.5	85.1	1.1	2702
Natural gas	2553	>2652.5	84.8	3.0	2633
Winkler oxygen	2523	2652.5	84.4	3.0	2583
Winkler air	2335	>2652.5	80.4	3.0	2397

It should be noted that these calculation in no way imply that this, or any other unit, could economically be retrofitting to burn these test fuels. Several other factors in addition to unit efficiency must be considered in an actual retrofit study. Two of these important factors are 1) redistribution of heat absorption between boiler, primary and secondary superheater, and reheat and economizer surface (a significant redistribution of which will affect metal temperatures, spray flows, and circulation); and, 2) changes in combustion-air and flue-gas weight from the original design quantities, which will affect fan and air heater performance. Both of these factors can have a significant influence on the feasibility of retrofitting existing units designed for conventional fossil fuel firing.

To aid in determining the value of the experimental data, B&W reran their design calculation without using the experimental results as input. The new inputs required for the computer program were the fuel composition and the desired temperature of combustion products leaving the air heater. The results of these calculations for the gas temperature and emissivity at the exit of the radiant furnace section are listed in Table 8. The combustion products temperature leaving the radiant section shows excellent agreement with the experimental values. This provides substantiation on how realistically the pilot-scale test furnace was able to model the radiant section of a utility boiler.

Comparing the gas emissivities of the combustion products at the radiant section exit as measured by IGT to those calculated by B&W reveals a large difference. This difference can be understood by looking at the emissivities dependent variables. These variables are the partial pressure of the radiating gas, the temperature of the gas mixture, and the distance across (beam length) the radiating gas. The temperature and partial pressure of the radiating gases are similar for the IGT test data and the B&W calculated values. Therefore the difference between the pilot-scale furance and the 360-MW boiler is due to the different beam length, 4 feet and 22 feet, respectively.

Table 8. CALCULATED AND MEASURED RADIANT SECTION EXIT GAS TEMPERATURES AND EMISSIVITIES

Fuel	IGT[a]		B&W[b]	
	T_g	ϵ_g	T_g	ϵ_g
Natural gas	2553	0.18	2633	0.29
Winkler oxygen	2523	0.22	2583	0.35
Winkler air	2335	0.17	2397	0.31
Koppers-Totzek oxygen	2554	0.19	--	--
Koppers-Totzek oxygen, 800 °F	2592	0.19	--	--
Koppers-Totzek oxygen, 800 °F plus 15% FGR	2681	0.22	--	--

[a] Experimental data collected on pilot-scale test furnace.

[b] Calculated values based on normal design technique.

MATHEMATICAL MODEL OF FURNACE PERFORMANCE

To allow the experimental data to be accurately extrapolated, a mathematical model was sought that would provide estimates of temperature and emissivity in agreement with the experimental results. In addition, the model had to be easy to use (not requiring a high-speed computer) yet provide reliable estimates. The method selected to compare the experimental results with those calculated by B&W is the "speckled-wall" model (SWM) developed by Hottel.[4] This model makes use of the follow assumptions:

1. The combustion products and flame in the combustion chamber are assigned a single mean temperature; this means that the furnace is treated as a well stirred reactor.
2. The gas is gray.
3. The heat sink surface area is gray and can be assigned a single temperature.
4. External losses through the furnace walls are negligible, and internal convection to the refractory furance walls can be neglected.
5. The arrangement of heat sink and refractory surfaces is such that any point on the furnace walls has the same view-factor to sink surfaces as any other point. This occurs only when the sink and refractory surfaces are intimately mixed. The walls are speckled.

The items of information needed to use the model applying the iterative method described below are the adiabatic flame temperature, the total enthalpy, the total surface area of the furnace, the ratio of sink surface area to refractory surface area, and the emissivity of the sink.

The model has the capability to –

1. Account for convective heat flux to the sink
2. Allow for heat losses through the furnace walls
3. Allow for the difference in flue-gas temperature and effective gas radiating temperatures, because an industrial furnace does not have perfect stirring.

The model gives substantially correct predictions of furnace performance for a wide variety of furnaces and can be expected to give a good comparison between fuels in a particular furnace.

---

[4] Hottel, H. C., J. Inst. Fuel 34: 220,1961.

A flame-to-sink energy exchange factor, $\overline{(GS)}_R$, for radiation heat transfer can be defined by –

$$\overline{(GS)}_R = A_T \left[\frac{A_T}{\varepsilon_s A_s} + \frac{1}{\varepsilon_g} - 1 \right]^{-1} \qquad (6)$$

for the case where the heat sink is well distributed. Here A_T is the total furnace area, A_s is the heat sink area, and ε_s and ε_g are the sink and flame emissivities, respectively. Then a total energy exchange factor can be defined to include radiative and convective heat transfer by –

$$\overline{(GS)}_{R,C} = (GS)_R + h_s A_s / 4\sigma T^3_{gs} \qquad (7)$$

where h_s is the convective heat-transfer coefficient, σ is the Stefan-Boltzman constant, and T_{gs} is the mean temperature between the sink and the flame.

A "reducing firing density" can be defined by –

$$D' = H_f / [\, \sigma \overline{(GS)}_{R,C} T_{AF}^4 \, (1 - T_o/T_{AF}) \,] \qquad (8)$$

where H_F is the total enthalpy input to the furnace and T_{AF} is a "pseudo-adiabatic" flame temperature defined as the temperature that the combustion products would attain if the total enthalpy input were used to heat the combustion products from ambient, T_o, at the mean heat capacity between T_o and the flame temperature. Combining the equation above with an energy balance and denoting the fraction of the input enthalpy transfer to the sink by η , we obtain –

$$\eta' D' + \tau^4 = (1 + \Delta' - \eta') \qquad (9)$$

where $\eta' = \eta(T_{AF} - T_o)/T_{AF}$

$\tau = T_s/T_{AF}$

and $\Delta' = \Delta/T_{AF}$

where Δ accounts for departures of the furnace from the well stirred approximation. The effective radiating temperature of the gas will differ from the mean enthalpy temperature of the gases at the flue of the furnace by an amount Δ, which depends on the firing density and furnace geometry.

The first attempt at using the well stirred speckled-wall model ($\Delta' = 0$) was to evaluate how it would agree with IGT experimental data and the values calcuated by B&W. The measured and calculated efficiencies are plotted in Figure 38 versus adiabatic radiance. Adiabatic radiance is defined as the total radiant energy that would be emitted from the combustion products of a test fuel at the test fuel's adiabatic temperature. Figure 38 again illustrates how accurately the pilot-scale test furnace was able to model the radiant section of a utility boiler. Thus to get efficiencies calculated with the well stirred speckled-wall model to agree with the IGT test data would demonstrate the model's ability to predict performance of a utility boiler radiant section.

To allow the speckled-wall model to be used from a completely theoretical position with no experimental data needed, an iterative method was devised. A combustion-products gas temperture is estimated at the exit of the radiant section. From this temperature an emissivity is calculated using the Hottel-Sarofim charts. (Any technique for calculating emissivities can be used. The Hottel-Sarofim method was chosen based on the ease of calculation and the universal availability of the gas emissivity charts.) This emissivity is plugged into Equation 6 to evaluate the flame-to-sink energy exchange factor. This permits the total energy exchange factor, Equation 7, and the reduced firing density, Equation 8, to be calculated. A reduced furnace efficiency can then be determined by Equation 9. This reduced efficiency can be turned into a true furnace efficiency using Equation 10. Having the true furnace efficiency, the exit-gas temperature can be determined using the heat content of the combustion-product gases. If the exit-gas temperature derived from the speckled-wall model agrees with the temperature used to calculate the emissivity, then the solution is

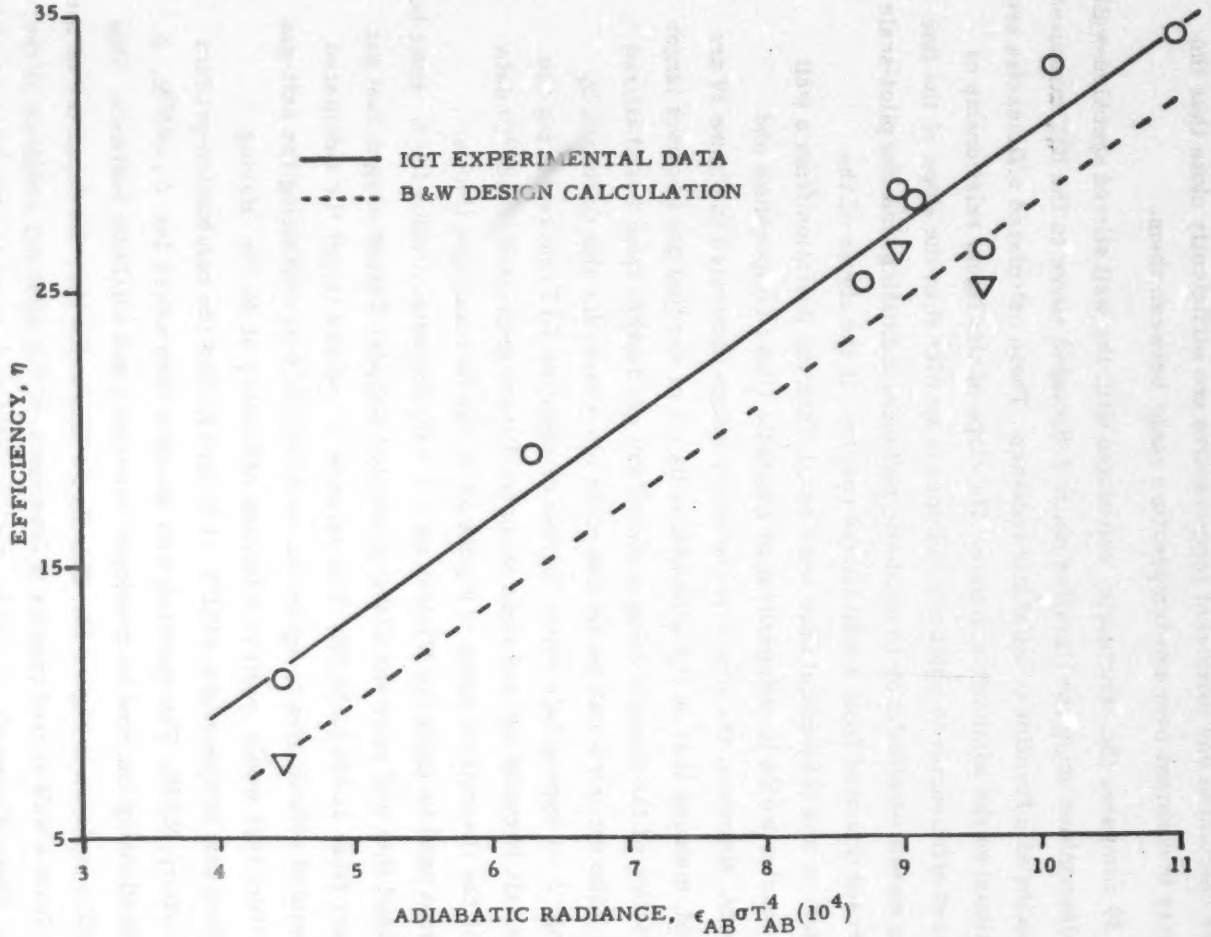

Figure 38. Comparison of IGT experimental and B&W calculated furnace efficiencies

finalized. If the temperature does not agree, then the estimated temperature is incremented, a new emissivity is calculated and plugged into the speckled-wall model, and the iteration continues. The procedure is followed until a satisfactory agreement between estimated and calculated temperatures is achieved, that is, until the calculated and estimated temperatures are sufficiently close that the emissivity is constant over the temperature range between them.

Figure 39 compares the efficiencies calculated with the well stirred speckled-wall model determined using the iterative method discussed above to the IGT measured efficiencies as a function of adiabatic radiance. These calculated efficiencies are proportional to the adiabatic radiance. The slope of this linear relationship of calculated efficiencies to adiabatic radiance is smaller than the slope of the line relating measured efficiency to adiabatic radiance, indicating that the pilot-scale test furnace deviated from a well stirred reactor. If the slopes of the experimental and theoretical lines were equal, then the deviation from a well stirred reactor would be independent of adiabatic flame temperature and emissivity. However, the slopes of the relationships illustrated in Figure 39 are not equal, meaning that as the adiabatic radiance of the fuel gas becomes larger the deviation of the furnace being modeled will get farther from a well stirred reactor. The speckled-wall model can make allowances for this deviation by assigning Δ an appropriate value. (Refer to Equation 9.) From reviewing the extreme left (Winkler air) and right (Koppers-Totzek preheated to 425°C) data points of the theoretical curve of Figure 39, it can be concluded that no connection need be made for Winkler air ($\Delta = 0$); however, a value for Δ must be determined that will raise the 425°C preheated Koppers-Totzek oxygen fuel gas efficiency from 22.9% to 34.2%. The value of Δ needed to get the calculated and measured efficiencies to agree can be determined by evaluating the exit-gas temperature that would result in a furnace efficiency of 34.2%. Having determined this temperature, 2592°F, it is used to find the combustion-product gas emissivity, 0.359. The speckled-wall model is then solved for Δ, 605°R. A linear relationship can now be developed between Δ and adiabatic radiance. This relationship is shown in Figure 40. This figure illustrates that the departure of the furnace from a well stirred reactor is dependent on the adiabatic radiance of the fuel gas. Using Figure 40, Δ can be determined for each of the fuel gases tested. This allows the efficiency for each fuel gas to be reevaluated using this non-well stirred speckled-wall model. As with the well stirred model, the iterative

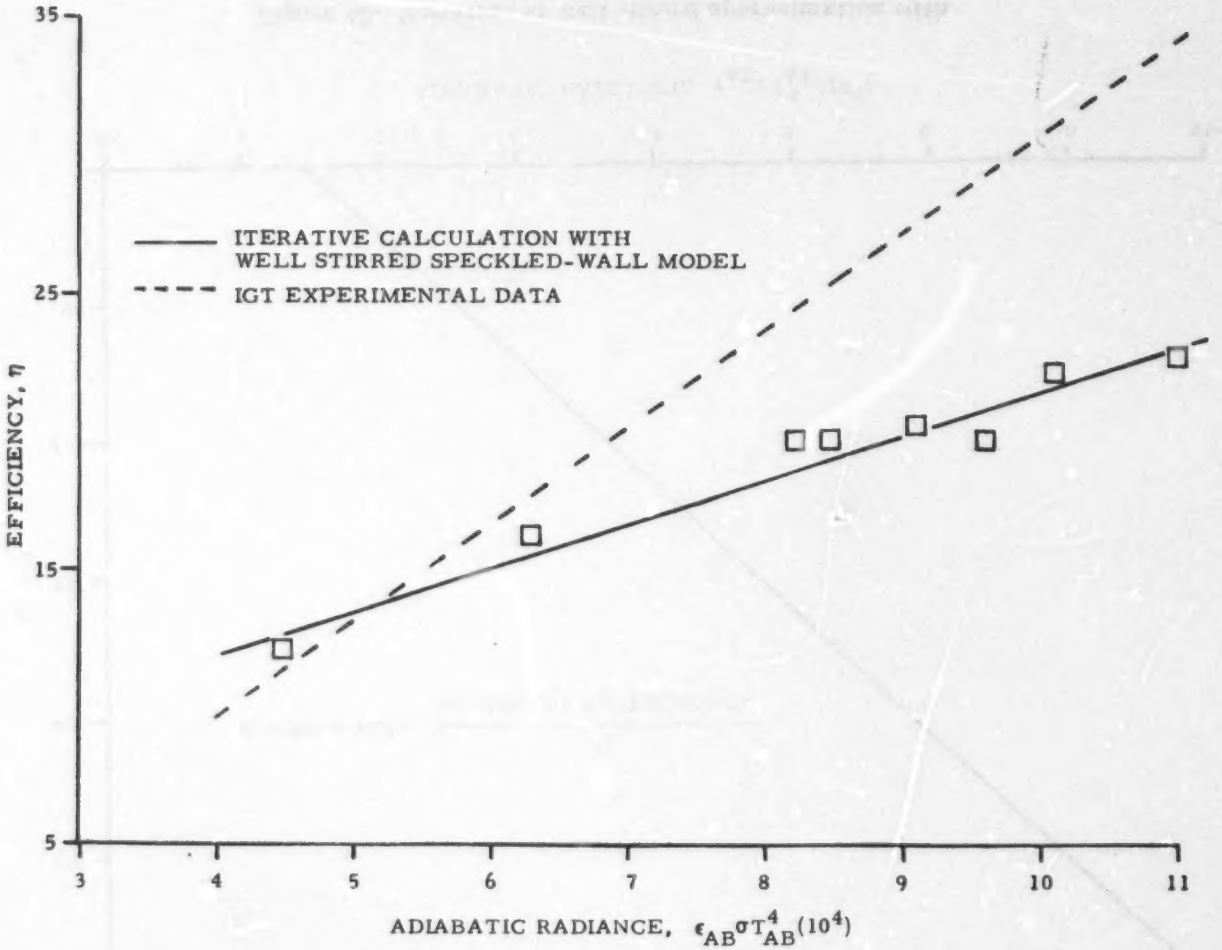

Figure 39. Comparison of experimental and well stirred speckled-wall model calculated furnace efficiencies

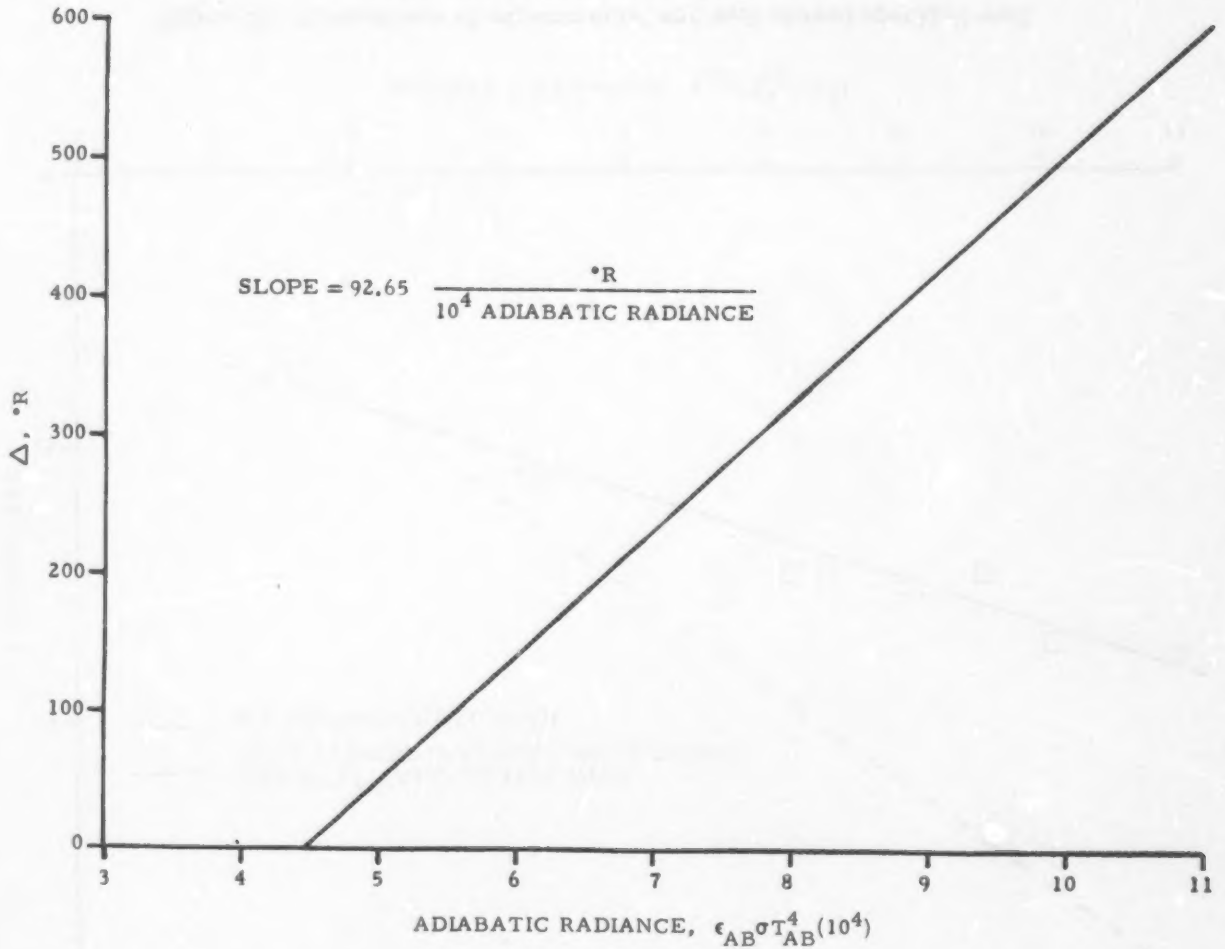

Figure 40. Variation of well stirred approximation with adiabatic radiance

procedure is followed. The results of this calculation are shown in Figure 41, and are listed in Table 9. The figure illustrates that the iterative speckled-wall calculation can give results in good agreement with the experiment when properly modified to allow for deviation of the furnace from perfect stirring. Table 10 lists the iteratively evaluated emissivities as well as those calculated by B&W. To evaluate the effect emissivity has on efficiency, the emissivity calculated by B&W for Winkler oxygen fuel gas was substituted in the non-well stirred speckled-wall model to determine an exit-gas temperature. The non-well stirred speckled-wall model using the B&W computed emissivity yields an exit-gas temperature of 2463°F, or 33°F above that determined using the iterative technique. Thus a 7.9% change in gas emissivity will produce only a 1.4% change in exit-gas temperature.

The non-well stirred speckled-wall model provides a calculation tool that yields good agreement with the more sophisticated techniques employed by B&W. Using the iterative technique, accurate predictions of furnace performance can be made for nonluminous fuels.

IN-THE-FLAME ANALYSIS

Detailed in-the-flame data were collected for natural gas preheated Koppers-Totzek and preheated Koppers-Totzek with 15% FGR. These data are to aid in quantitative modeling of large-scale turbulent diffusion flames and to provide a qualitative guide in understanding and controlling NO emission levels. These measurements included gas species concentrations and temperature profiles. A supplement volume containing these detailed in-the-flame data is available upon request from the EPA project officer,(919) 541-2236.

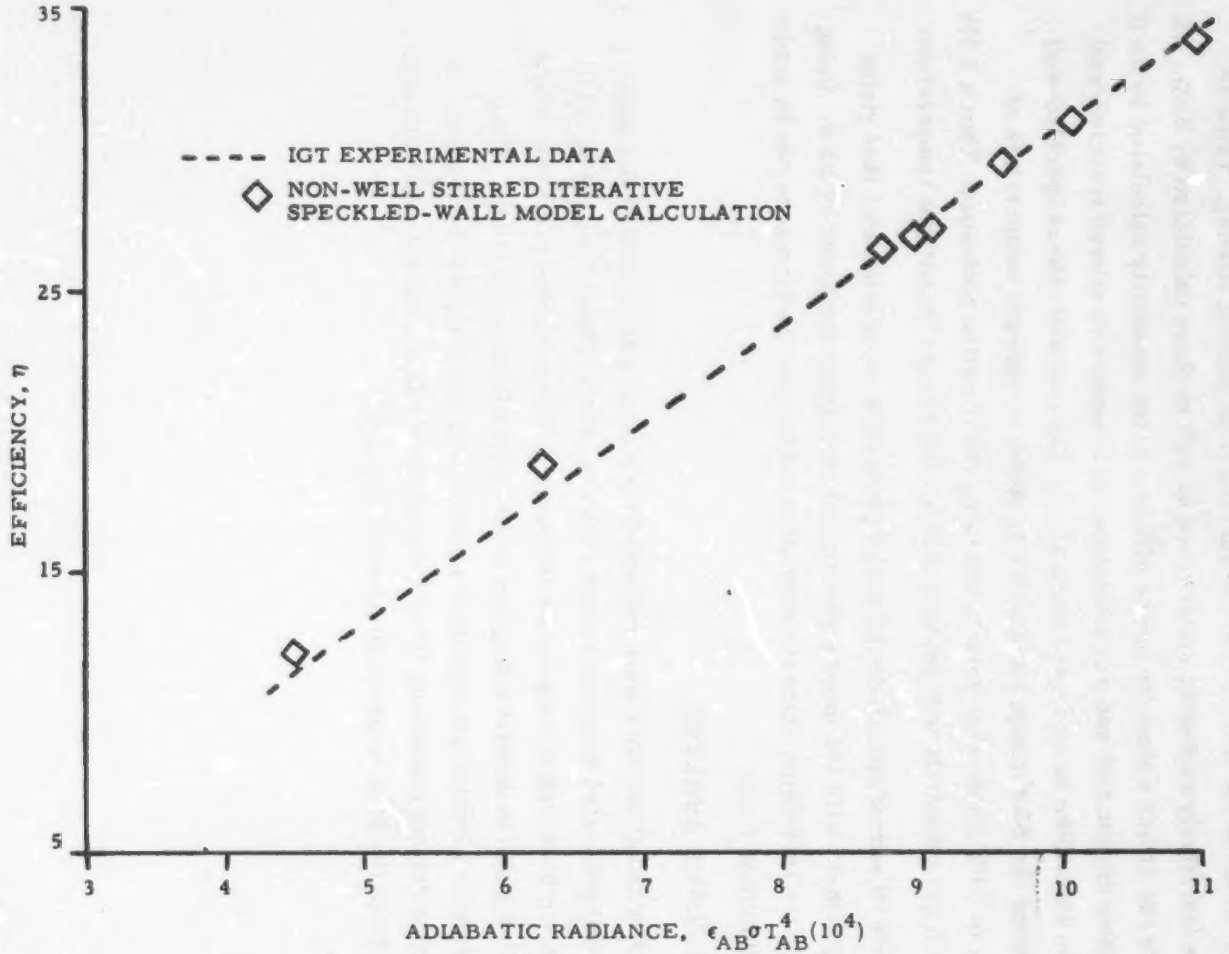

Figure 41. Comparison of experimental and non-well stirred speckled-wall model calculated furnace efficiencies

Table 9. COMPARISON OF MEASURED AND CALCULATED FURNACE EFFICIENCIES

Fuel	$\epsilon_A \sigma T_A^4 (10^4)$	IGT[a]	B&W[b]	SWM[c]	NSWM[d]
Natural gas	8.98	28.6	26.3	19.8	27.0
Lurgi oxygen	8.72	25.2	--	19.8	26.6
Winkler oxygen	9.61	26.4	25.1	19.9	29.6
Koppers-Totzek oxygen	10.12	33.1	--	22.4	31.4
Wellman-Galusha air	6.31	19.0	--	16.3	18.9
Winkler air	4.47	10.8	7.8	12.2	12.2
Koppers-Totzek oxygen, 425°C	11.00	34.2	--	22.9	34.2
Koppers-Totzek oxygen, 425°C plus 15% FGR	9.10	28.2	--	20.4	27.4

[a] Measured on IGT pilot-scale test furnace.

[b] Calculated by B&W for Teche Station Boiler (RB-455) using design calculation technique.

[c] Calculated using the well stirred iterative speckled-wall model ($\Delta = 0°R$).

[d] Calculated using the non-well stirred iterative speckled-wall model (Δ evaluated using Figure 67).

Table 10. COMPARISON OF CALCULATED EMISSIVITIES

Fuel	B&W[a]	SWM[b]	NSWM[c]
Natural gas	0.29	0.30	0.33
Winkler oxygen	0.35	0.35	0.38
Winkler air	0.31	0.34	0.34

[a] Calculated by B&W for Teche Station Boiler (RB-455) using design calculation technique.

[b] Calculated using the well stirred iterative speckled-wall model technique ($\Delta = 0°R$).

[c] Calculated using the non-well stirred iterative speckled-wall model technique (Δ evaluated using Figure 67).

CONVERSION TABLE

ENGLISH TO SI METRIC CONVERSION FACTORS

To Convert From	To	Multiply By
$lb/10^6$ Btu	ng/J	4.299 E + 02
10^6 Btu/hr	MWt	2.928751 E − 01
Btu	J	1.055 E E + 03
psi	Pa	6.894757 E + 03
SCFH	m^3/s	7.865790 E − 06
ft/s	m/s	3.048000 E − 01
Inch	m	2.540000 E − 02
Feet	m	3.048000 E − 01
$Feet^2$	m^2	9.290304 E − 02
Inches of water (pressure)	Pa	2.4884 E + 01
lb/ft^3	kg/m^3	1.601846 E + 01
gpm	m^3/s	6.309020 E − 05
$Inch^2$	m^2	6.451600 E − 04
°F	°C	$t°C = (t°F - 32)/1.8$
°R	°C	$t°C = [(5/9)t°R] - 273.15$

J = Joule
g = gram
s = second
MWt = megawatts thermal
gpm = gallons (U. S. liquid)/minute
Pa = Pascal
m = metre
k = kilo (10^3)
n = nano (10^{-9})
M = mega (10^6)
C = Celsius
F = Fahrenheit
R = Rankine
psi = pounds per square inch
SCFH = standard cubic feet per hour